CHEMISTRY
A European Journal

A Journal of
ChemPubSoc Europe

Accepted Article

Title: Gold(I) NHC Complexes: Antiproliferative Activity, Cellular Uptake, Inhibition of Mammalian and Bacterial Thioredoxin Reductases, and Gram-positive directed Antibacterial Effects

Authors: Claudia Schmidt, Bianka Karge, Rainer Misgeld, Aram Prokop, Raimo Franke, Mark Brönstrup, and Ingo Ott

To be cited as: *Chem. Eur. J.* 10.1002/chem.201604512

Link to VoR: http://dx.doi.org/10.1002/chem.201604512

Supported by
ACES

WILEY-VCH

10.1002/chem.201604512

Gold(I) NHC Complexes: Antiproliferative Activity, Cellular Uptake, Inhibition of Mammalian and Bacterial Thioredoxin Reductases, and Gram-positive directed Antibacterial Effects

Claudia Schmidt[1], Bianka Karge[2], Rainer Misgeld[3], Aram Prokop[3], Raimo Franke[2], Mark Brönstrup[2] and Ingo Ott[1]

[1]Institute of Medicinal and Pharmaceutical Chemistry, Technische Universität Braunschweig, Beethovenstrasse 55, 38106 Braunschweig, Germany; [2]Department of Chemical Biology, Helmholtz Centre for Infection Research GmbH, Inhoffenstrasse 7, 38124 Braunschweig, Germany; [3] Department of Paedriatric Oncology, Children's Hospital Cologne, Amsterdamer Strasse 59, 50735 Cologne, Germany

Corresponding author information
Prof. Dr. Ingo Ott, Email: ingo.ott@tu-bs.de, Tel.: +49 531 3912743

Keywords: antibacterial, anticancer, atomic absorption spectroscopy, cellular uptake, drug resistance, gold complexes, high resolution continuum source molecule absorption spectroscopy, *N*-heterocyclic carbenes, thioredoxin reductase

10.1002/chem.201604512

Abstract

Gold complexes with *N*-heterocyclic carbene (NHC) ligands represent a promising class of metallodrugs for the treatment of cancer or infectious diseases. In this report, the synthesis and the biological evaluation of halogen-containing NHC-Au(I)-Cl complexes are described. The complexes **1** and **5a**-**5f** displayed good cytotoxic activity against tumor cells, and cellular uptake studies suggested that an intact Au-NHC fragment is essential for the accumulation of high amounts of both the metal and the NHC ligand. However, the bioavailability was negatively affected by serum components of the cell culture media and was influenced by likely transformations of the complex. One example (**5d**) efficiently induced apoptosis in vincristine- and daunorubicin-resistant P-glycoprotein overexpressing Nalm-6 leukemia cells. Cellular uptake studies with this compound showed that both the wildtype and resistant Nalm-6 cells accumulated comparable amounts of gold, indicating that the gold drug was not excreted by P-glycoprotein or other efflux transporters. The effective inhibition of mammalian and bacterial thioredoxin reductases (TrxR) was confirmed for all gold complexes. Antibacterial screening of the gold complexes afforded a particular high activity against Gram-positive strains, reflecting their high dependence on an intact Trx/TrxR system. This result is of particular interest as the inhibition of bacterial TrxR represents a comparably little explored mechanism of new anti-infectives.

10.1002/chem.201604512

Introduction

The interest in using gold and its complexes dates back to ancient times and also was an important aspect of alchemy in medieval Europe and in the Renaissance period, when gold was an essential ingredient of so-called *aurum vitae* medicines.[1] Early scientific reports by Robert Koch demonstrated antibacterial activities of gold cyanide salts,[2] and with the contributions of Forestier,[3] gold complexes found their way into modern drug therapy. Currently, gold-based drugs like Auranofin are still in use for the treatment of symptoms of rheumatoid arthritis. More recently the possible therapeutic impact of gold complexes has caught the attention of inorganic medicinal chemistry due to their strong effects against the growth of cancer cells and pathogenic bacteria.[4]

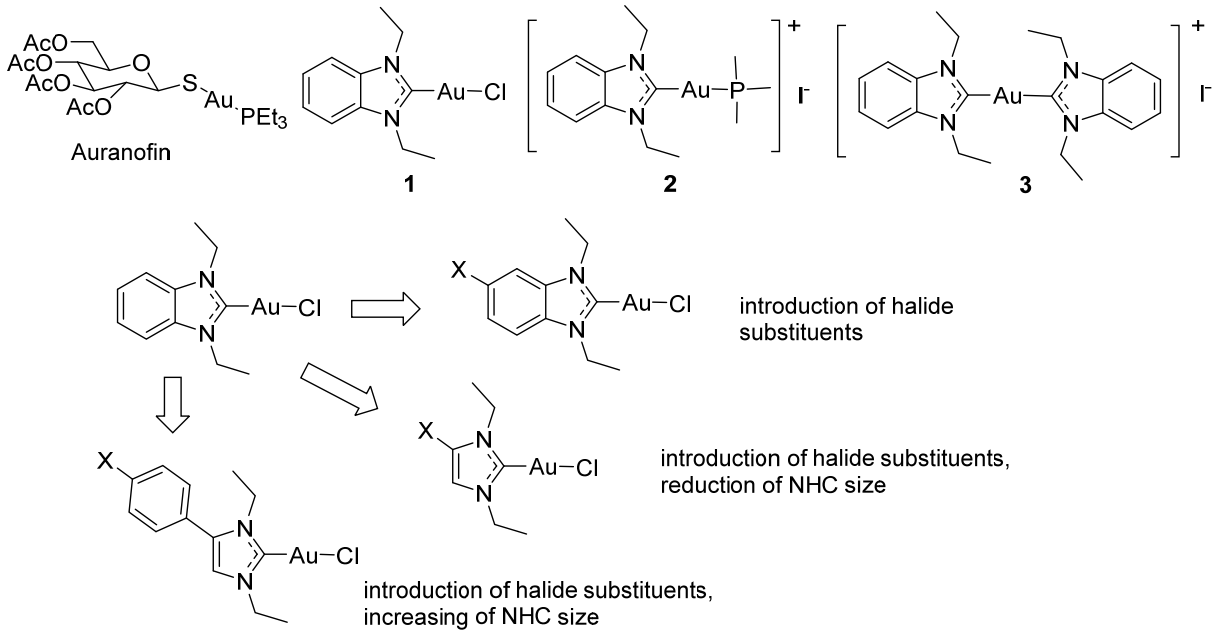

Figure 1: Examples of previously studied gold(I) NHC complexes and strategy for metallodrug design

One class of gold complexes with high potential as drug leads is formed by complexes with *N*-heterocyclic carbene (NHC) ligands.[5] This organometallic scaffold offers distinct advantages over traditional gold complexes due to its improved stability and the structural versatility of the NHC ligand that allows the convenient synthesis of larger pools of complexes for the optimization of lead properties. Different types of gold NHC complexes have been investigated as anticancer and antibacterial agents, containing gold in the oxidation states +1 and +3 and further coordinated ligands such as halides or phosphanes (see Figure 1 for a few selected examples).[6] Concerning their mode of drug action, several molecular targets and affected biochemical pathways have been identified, including thioredoxin reductase enzymes, the zinc-finger enzyme PARP-1, G-quadruplexes, or mitochondrial respiration.[6a-d, 6f, i, k, 7] The relevance of the respective targets and pathways was found to depend on the type of complex as well as the nature of the coordinated ligands.

10.1002/chem.201604512

For example, activation by reduction through cellular sulfides was confirmed for gold(III)-complexes,[6j] while for gold(I)-containing cationic lipophilic complexes[6f, h, i] enhanced effects against mitochondria were noted. In recent publications we reported on gold(I) complexes containing a benzimidazolylidene-derived NHC ligand of the general type (NHC)Au(I)L (NHC: -triaryl/trialkylphosphane L: -Cl) as thioredoxin reductase inhibitors and antiproliferative agents.[6b-d, 6g, h, k, 7] Selected complexes were studied pharmacologically in much detail, which further confirmed the general relevance of TrxR inhibition and interference with mitochondrial pathways for the triggering of antiproliferative effects and apoptosis induction. For example, a disruption of the interaction of Trx with ASK1 and a subsequent activation of p38-associated signaling was observed for complex **3**.[6d]

Further development of gold(I) NHC complexes would now benefit from systematic structure-activity relationships (SAR) through an extension of the pool of investigated compounds and their profiling in target-based assays (inhibition of TrxR), phenotypic assays (inhibition of cellular proliferation) and the correlation of the two parameters through intracellular concentration measurements. With this in mind, we have prepared a series of halogen-containing derivatives (Cl as coordinated ligand, F and Br as substituents on the NHC part) and varied the benzimidazole NHC backbone (see Figure 1). In particular, the introduction of halogen substituents on the NHC core appeared promising for modulating lipophilicity and addressing additional molecular interactions such as halogen bonding.[8]

Motivated by recent reports on anti-infective properties of gold(I) NHC complexes,[9] as well as the renewed interest in Auranofin as an antibacterial and antiparasitic agent[10], we have extended our investigations towards screening of the complexes as possible TrxR-inhibiting antibacterial agents.

Results

Chemistry

The synthesis of the target compounds followed established procedures with appropriate minor modifications.[6h, k, 11] Initially the (benz)imidazolium cations **4a**-**g** were formed by reacting the respective (benz)imidazoles with ethyl iodide under presence of a base (Scheme 1). Complexes of the type (NHC)Au(I)Cl **5a**-**g** could be obtained by reaction of the (benz)imidazolium cations **4a**-**g** with silveroxide, followed by a transmetallation reaction using Chlorido(dimethylsulfide)gold(I). All complexes were characterized by ^{1}H-, ^{13}C-NMR, and MS spectroscopy, and the high purity of all target compounds was confirmed by elemental analysis. ^{19}F-NMR spectra were recorded for the fluorinated compounds **4a**, **4f**, **5a** and **5f**. The obtained spectroscopic data were consistent with the proposed structures.

10.1002/chem.201604512

Mass spectrometry confirmed presence of the respective $[M]^+$, $[M\text{-}Cl]^+$ and $[M\text{-}I]^+$ ions, and mass spectra also showed the expected isotope patterns for bromine- or chlorine-containing compounds.

In the ^{1}H- and ^{13}C-NMR spectra some characteristic changes upon complex formation were observed. Expectedly, the signals of the hydrogen at position 2 of the (benz)imidazole cations in the ^{1}H-NMR spectra of **4a**-**g** disappeared upon gold coordination in **5a**-**g**. The absence of the proton at position 2 in the (phenyl)imidazole derivatives **5c**-**g** was further reflected by missing $^4J_{H2\text{-}H5}$ couplings, which were present in their synthesis precursors **4c**-**g**.

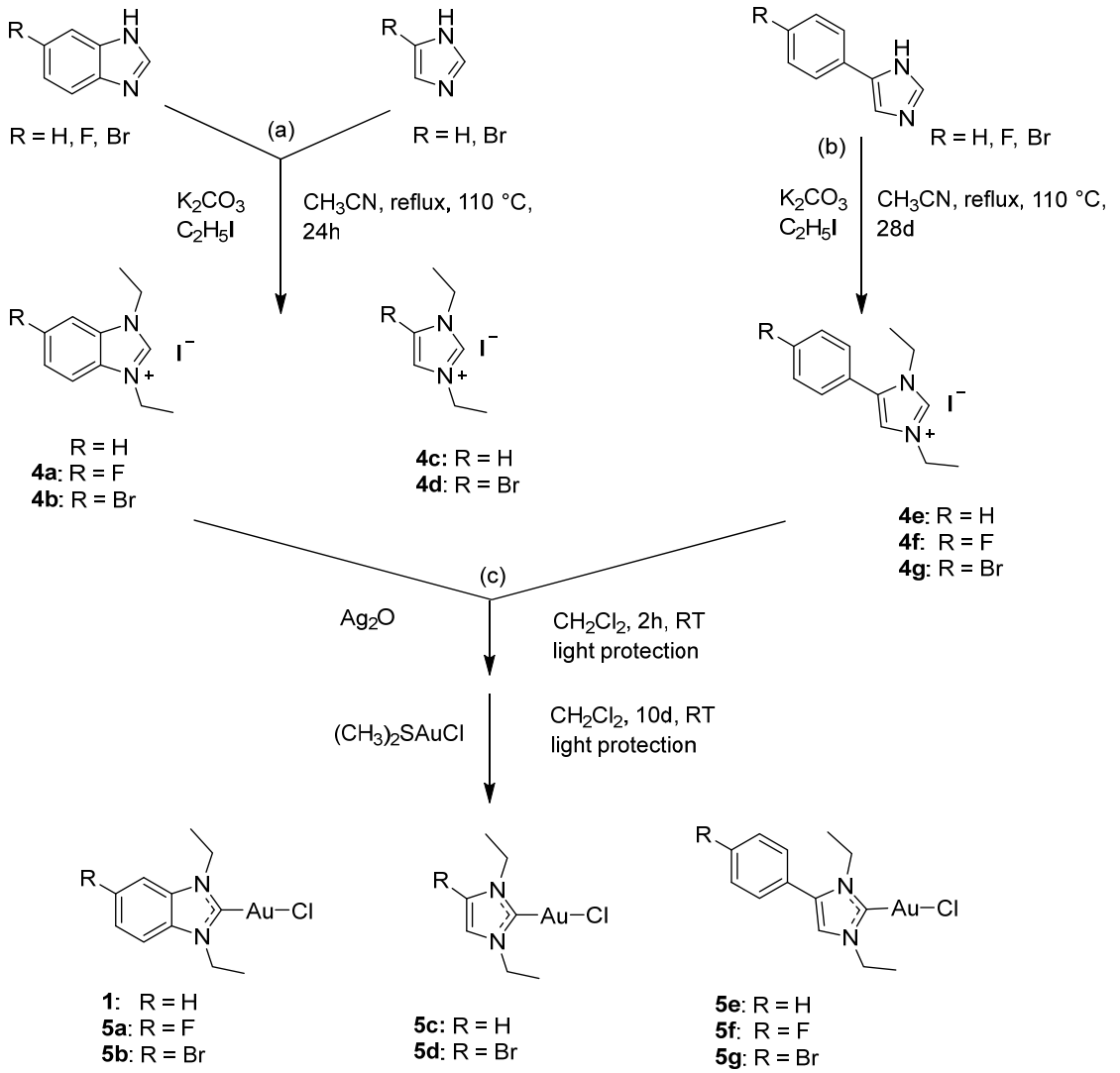

Scheme 1: Synthesis of the target compounds: (a) Synthesis of imidazolium and benzimidazolium ligands, (b) Synthesis of phenylimidazolium ligands, (c) Synthesis of NHC-Au-Cl complexes.

In the imidazole NHC complexes **5c**-**g** the signals of the proton at C5 of the imidazole ring were shifted upfield 0.4 – 0.7 ppm compared to the respective imidazolium precursor cations **4c**-**g**. Moreover, the aromatic hydrogens of the NHC ligands of **5a**-**g** showed an upfield shift of up to 0.45 ppm relative to the respective signals of the precursor cations **4a**-**g**. In the ^{13}C

10.1002/chem.201604512

NMR spectra of complexes **5a**-**g** the signal for the carbon at position 2, which is coordinated to gold(I), is observed at significantly higher ppm values (34 ppm in case of imidazole derivatives and 36 ppm in case of benzimidazole derivatives) than the corresponding signals of **4a-g.** Carbon-fluorine $J_{C,F}$ couplings over up to 4 bonds could be observed in the fluorine containing compounds.

Antiproliferative effects

The tumor cell growth inhibitory effects of complexes **5a**-**g** were determined in HT-29 colon carcinoma, as well as MCF-7 and MDA-MB-231 breast cancer cells (see Table 1). RC-124 human kidney cells were used as a non-tumor reference cell line, and Auranofin and AuCl served as references for gold complexes. Complexes **1** and **5a**-**g** triggered IC_{50} values in the rather narrow range of 4 – 17 µM. A bioselectivity for the tumor cells was not observed for any of the complexes, since RC-124 cells were affected within the same concentration range. A certain trend for higher cytotoxicity may be noted for the fluorinated derivatives **5a** and **5f** and the phenylimidazole derived complex **5e**, which showed the strongest antiproliferative effects in all cell lines. The reference compound Auranofin remained the most active gold complex in all cell lines, whereas the gold free ligands **4a**-**g** as well as AuCl were inactive (IC_{50} values > 100 µM in all cases).

Compound	HT-29	MCF-7	MDA-MB-231	RC-124
Auranofin	$3.79^{+/-0.18}$	$2.00^{+/-0.05}$	$1.54^{+/-0.12}$	$1.44^{+/-0.03}$
AuCl	> 100	> 100	>100	> 100
Ligands (**4a-g**)	> 100	> 100	> 100	> 100
1	$11.15^{+/-0.71}$	$6.68^{+/-0.82}$	$9.18^{+/-0.50}$	$5.07^{+/-0.14}$
5a	$6.23^{+/-0.57}$	$4.73^{+/-0.65}$	$7.20^{+/-0.45}$	$4.91^{+/-0.73}$
5b	$11.71^{+/-0.41}$	$7.19^{+/-0.83}$	$9.00^{+/-0.69}$	$11.48^{+/-0.45}$
5c	$16.97^{+/-0.25}$	$11.25^{+/-1.09}$	$11.58^{+/-1.03}$	$10.58^{+/-0.69}$
5d	$12.05^{+/-0.72}$	$6.52^{+/-0.47}$	$8.22^{+/-0.37}$	$5.49^{+/-0.32}$
5e	$6.80^{+/-0.98}$	$4.76^{+/-0.21}$	$8.13^{+/-0.60}$	$4.46^{+/-0.04}$
5f	$6.14^{+/-0.75}$	$5.05^{+/-0.67}$	$5.54^{+/-0.25}$	$4.62^{+/-0.25}$
5g	$11.59^{+/-1.51}$	$9.05^{+/-1.88}$	$10.89^{+/-0.15}$	$8.84^{+/-0.33}$

Table 1: Antiproliferative effects of Auranofin, AuCl, ligands **4a**-**g** and compounds **5a**-**g** expressed as IC_{50} values (µM) with standard errors as superscripts

Protein binding and cellular uptake into tumor cells

Previous studies had indicated that the extent of the cytotoxic activity of gold(I) NHC complexes is strongly influenced by the efficiency of their accumulation in cells and that in the case of (NHC)Au(I)Cl complexes their cellular bioavailability is affected by binding to

10.1002/chem.201604512

albumin.[6h] Complexes **5e**-**g** were selected for evaluation of the protein binding and cellular accumulation as they represent examples with high cytotoxic activity.

Initially, the binding to proteins of fetal calf serum was determined with a precipitation assay and afforded values > 80 % for **5e**-**g** (see Figure 2). Similar experiments using albumin showed complete binding (100 %, see supporting information).

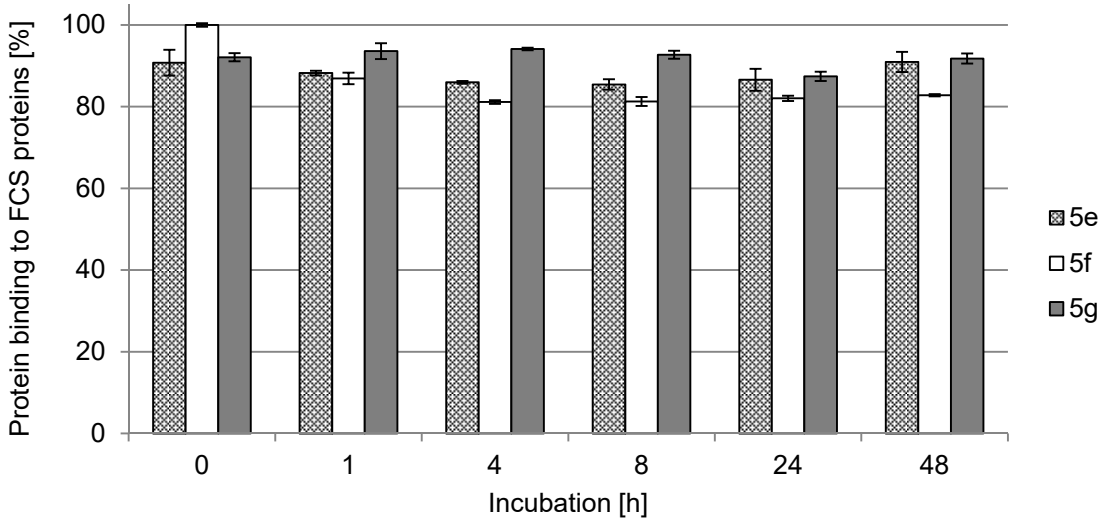

Figure 2: Binding to proteins of fetal calf serum by **5e**-**5g**

To assess the cellular uptake of the complexes, the gold levels in MCF-7 cells were determined by high resolution continuum source atomic absorption spectroscopy (HR-CS AAS) after exposure to 12.0 µM of **5e**-**g** over a period of 48h. The experiments were performed under routine cell culture conditions (medium supplemented with FCS, see Figure 3a) as well as under serum-free conditions (see Figure 3b) to allow conclusions on the influence of the strong protein binding of the complexes. In the experiments using serum containing cell culture media all complexes afforded well detectable gold levels, however, the uptake of **5e** was substantially higher than that of **5f** and **5g** (see Figure 3b). Since all three complexes had shown a very high protein binding, it can be speculated that in the competition between cellular uptake and binding to proteins the halide substituents of **5f** and **5g** might direct the complexes towards the proteins whereas in the case of **5e** cellular accumulation is the stronger preferred route. Notably, **5e** is less lipophilic than **5f** and **5g** as determined by measuring the log P values (see supporting information). The negative effect of halide substituents on the cellular uptake could be further confirmed in analogous reference experiments with the imidazole derived compounds **5c** and **5d** where the bromine containing **5d** showed a lower accumulation than **5c**. (see supporting information).

In the experiments using serum free cell culture media complexes **5e**-**f** showed comparable cellular gold levels during the first 8 hours of the exposure, which further confirmed the negative influence of serum on the uptake of the gold complexes. After longer incubation

10.1002/chem.201604512

(24h and 48h), however, the cellular levels of **5f** and **5g** were again substantially lower compared to those of **5e**. This might indicate that gold is exported from the cells after a decomposition or metabolisation of **5f** and **5g**.

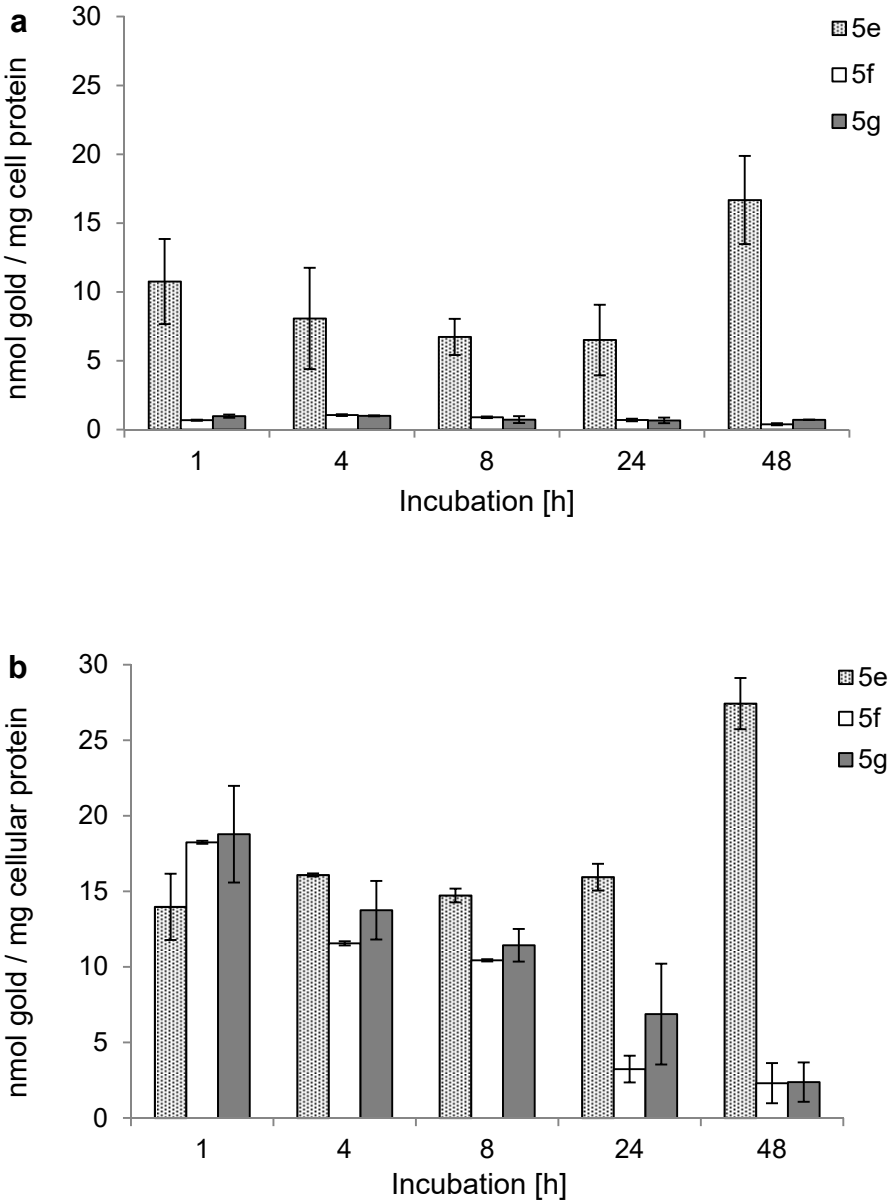

Figure 3: Cellular gold uptake into MCF-7 cells exposed to 12.0 µM of complexes **5e**-**g**; a) experiments with serum containing cell culture media; b) experiments with serum free cell culture media

Fluorine can be measured with high sensitivity using the HR-CS AAS technology.[12] For this purpose gallium is added as a modifier to the probes. The absorbance of a GaF diatomic species, which is formed upon heating in the AAS graphite tube, can be measured and used for the sensitive and selective detection of fluorine in biological samples. The underlying methodology is commonly referred to as HR-CS MAS.

10.1002/chem.201604512

Here we used the HR-CS MAS technology to quantify fluorine in the same samples of cells exposed to **5f**, which had been used for gold quantification. Additionally, the synthesis precursors and possible decomposition products AuCl and **4f** were included in the experiments (see Figure 4).

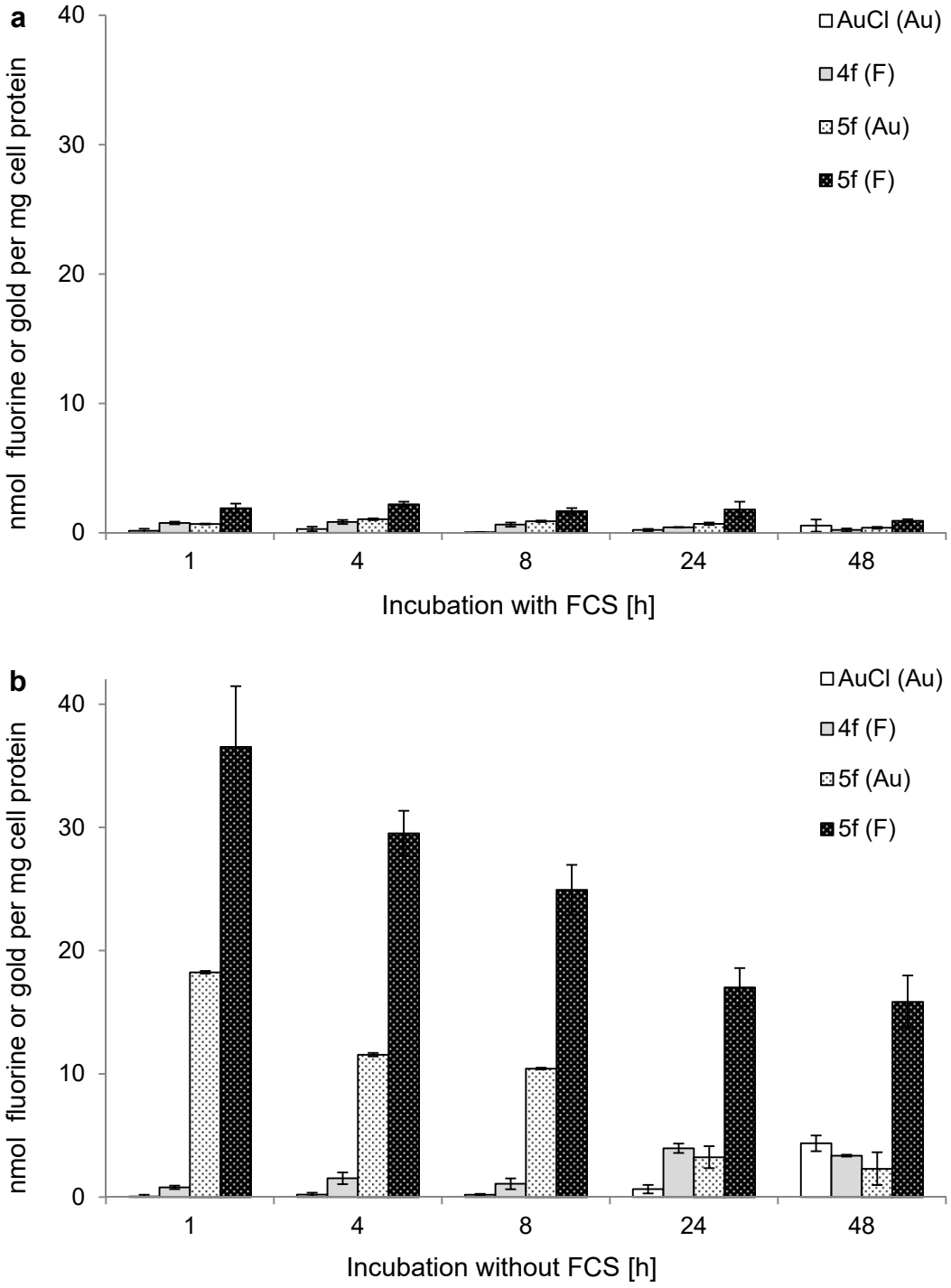

Figure 4: Cellular fluorine and gold levles in MCF-7 cells exposed to 12.0 µM of AuCl, **4f** and **5f**; a) experiments with serum containing cell culture media (a version of figure 4a with different scaling of the y-axis is provided in the supporting information; b) experiments with serum free cell culture media

10.1002/chem.201604512

The most striking result from these investigations was that under serum free conditions the cellular gold and fluorine levels with **5f** significantly exceeded those of the respective gold and fluorine containing reference compounds AuCl and **4f** for at least 24 hours. This strongly indicates that an intact complex (or an intact Au-NHC fragment) is required to accumulate high amounts of both gold and the NHC ligand in the cells. The uptake process occurred very fast (within 1h) and with extended incubation both gold and fluorine levels decreased continuously. Importantly, the fluorine levels determined with **5f** were significantly higher than the gold levels suggesting that **5f** is transformed or decomposes inside the cells. Under serum containing conditions as expected strongly decreased cellular gold and fluorine concentrations were found after exposure to **5f**. Also in this case gold and fluorine from **5f** were higher than those obtained with the respective references AuCl and **4f** (see figure 4a and supporting information).

Effects against drug resistant leukemia cells

Recently, we reported on the high activity of complex **1** against drug resistant leukemia cells.[6k] Here, the apoptosis-inducing activity of the structurally different complex **5d** was exemplarily investigated in daunorubicin and vincristine resistant Nalm-6 cells, which overexpress the drug efflux-transporter P-glycoprotein.[6h] In good agreement with the previous results on **1**, complex **5d** induced apoptosis in both resistant cell lines to a comparable extent as in the sensitive wildtype Nalm-6 cells in a concentrations of 5 µM and above. Additional experiments showed that the apoptosis induction was independent of Bcl-2 expression (experiments in human melanoma cells, see supporting information).

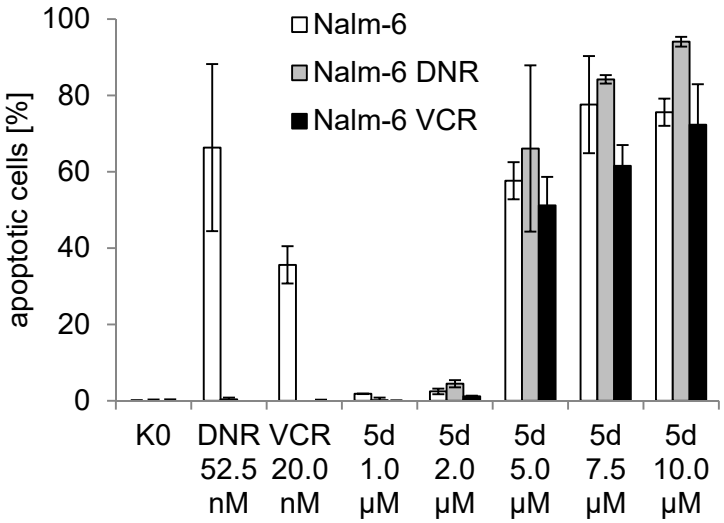

Figure 5: Apoptosis induction in Nalm-6 wildtype cells and Daunorubicine- (Nalm-6-DNR) and Vincristin- (Nalm-6-VCR) resistant Nalm-6 cells by **5d**; Co: untreated control, DNR 52.5 nM and VCR 20 nM: cells treated with daunorubicine or vincristin at the indicated concentrations

10.1002/chem.201604512

Since the resistance to daunorubicin and vincristine in Nalm-6 cells is likely dominated by the increased expression of P-glycoprotein, which leads to an enhanced efflux of toxic compounds, we evaluated the gold levels in both the drug resistant and wildtype cells after a 12h exposure to complex **5d** by HR-CS AAS. Concentrations of 3.0 and 12.0 µM were chosen according to the results of the apoptosis measurements, reflecting low and high apoptosis induction. Comparable gold levels were found in the resistant and wildtype cells, and the induction of apoptosis at higher exposure concentrations to **5d** was accompanied by elevated intracellular gold levels. The high correlation between the induction of apoptosis and the intracellular compound concentration in sensitive and resistant Nalm-6 subtypes strongly indicates that complex **5d** is not a substrate of the P-glycoprotein or other efflux transporter.

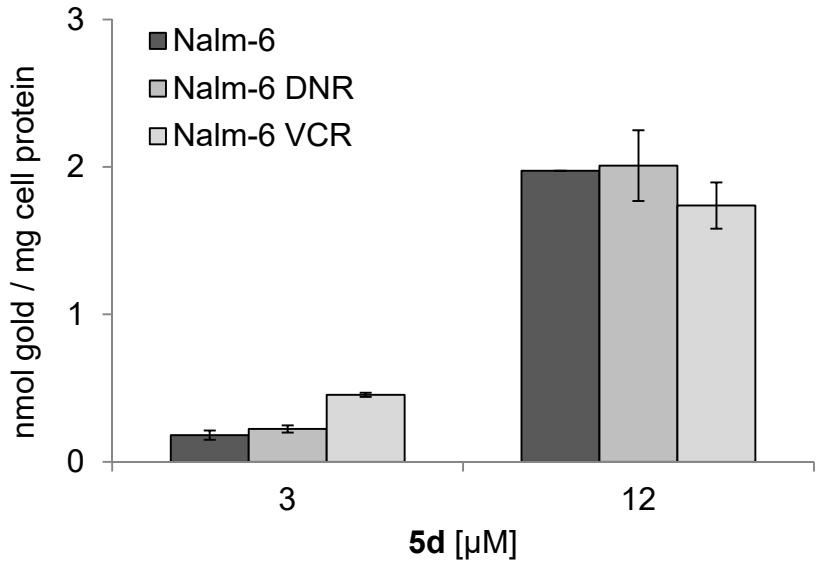

Figure 6: Cellular gold uptake into wildtype and resistant Nalm-6 cells exposed to complex **5d** after 12h

Antibacterial effects

As mentioned above, the antibacterial effects of gold complexes have recently triggered increased attention.[4e, 9a, 10a, c] Here, we screened complexes **1** and **5a**-**g** as well as Auranofin as inhibitors of bacterial growth in a number of Gram-negative (*A. baumannii, E. cloacae, E. coli, K. pneumoniae, P. aeruginosa*) and Gram-positive (*E. faecium* and *S. aureus*) bacteria (see Table 2), a collection known as the ESKAPE panel.[13] As growing resistances of the ESKAPE pathogens render antibiotic therapy increasingly difficult, the development of new antimicrobial agents acting against ESKAPE pathogens is urgently needed. The activities of the gold complexes were expressed as minimal inhibitory concentration (MIC) values, defined as the lowest concentration of an antibacterial compound that suppresses the visible growth of the microorganisms.

10.1002/chem.201604512

Overall, the Gram-positive *E. faecium* and *S. aureus* strains were inhibited at low micromolar concentrations by **1** and **5a**-**g**, whereas substantially lower efficacies against Gram-negative bacterial strains were observed. Compound **5c** exhibited moderate MIC values against *E. coli*, *E. cloacae* and *K. pneumoniae* in the range of 37-42 μM, activities that clearly exceeded that of the reference metallodrug Auranofin. The activities of **1** and **5a**-**g** against the Gram-positive strains were in a narrow range overall, although a consistent preference for complexes **1**, **5c** and **5d** was observed. The most potent analog **5d** inhibited *E. faecium* and two MRSA strains at MIC values of 3.12, 0.64 and 0.64 μM, respectively, activities that were superior to those of Auranofin (18.40, 2.25, 2.30 μM).

Compound	*A. baumannii*	*E. cloacae*	*E. coli*	*K. pneumoniae*
Auranofin	>73.58	>73.58	>73.58	>73.58
Antibiotic	2.41 +/-0.42(n=4)	0.24 +/-0.09(n=4)	<0.15	0.54 +/-0.18
1	>100	100 +/-0(n=4)	>100	>100
5a	>100	>100	>100	>100
5b	>100	66.67 +/-16.66	83.33 +/-16.66	>100
5c	>100	37.49 +/-7.21(n=4)	37.49 +/-12.51(n=2)	41.67 +/-8.33
5d	>100	66.66 +/-16.67	83.33 +/-16.67	83.33 +/-16.67
5e	>100	100 +/-0.00(n=4)	>100	>100
5f	>100	100 +/-0.00	100.00 +/-0.00	75.00 +/-25.01
5g	>100	>100	>100	>100

Compound	*P. aeruginosa*	*E. faecium*	MRSA1	MRSA2
Auranofin	>73.58	18.40	2.30 +/-0.00(n=2)	2.30
Antibiotic	11.05 +/-2.51	> 15.09	4.83 +/-4.65(n=2)	2.02 +/-0.59(n=4)
1	>100.	4.80 +/-1.48(n=4)	1.03 +/-0.27	1.94 +/-0.39(n=4)
5a	>100.	6.03 +/-0.00	2.61 +/-0.52	3.13 +/-1.55
5b	>100	8.34 +/-2.08	3.13 +/-0.00	4.16 +/-1.05
5c	>100	2.97 +/-1.18(n=4)	2.61 +/-0.53	2.55 +/-1.29(n=4)
5d	>100	3.12 +/-0.00	0.64 +/-0.14	0.64 +/-0.14
5e	>100	6.45 +/-2.40	5.20 +/-1.04	4.16 +/-1.04
5f	>100	12.49 +/-0.00	6.28 +/-0.00(n=2)	7.30 +/-2.75
5g	>100	12.51 +/-0.00	6.25 +/-0.00	6.25 +/-0.00

Table 2: Mean MIC values in μM +/- standard error of the mean (a table with μg/mL values can be found in the supporting information). Unless indicated otherwise: n=3 (Auranofin: n=1); MRSA = Methicillin-resistant *Staphylococcus aureus*. As positive control antibiotics, Amikacin (*P. aeruginosa*), Linezolid (*S. aureus*), and Ciprofloxacin (all other strains) have been used.

Inhibition of mammalian and bacterial TrxR

The inhibition of TrxRs by the gold complexes was investigated as a likely contributing factor for their bioactivity. In fact, mammalian TrxRs are considered as a relevant target for gold

10.1002/chem.201604512

NHC complexes[6f, k] ,however, their effects against bacterial TrxRs have not been investigated to the best of our knowledge. Isolated mammalian (rat liver) TrxR and bacterial TrxR from *E. coli* were used in established assay procedures for a comparative study of the enzyme inhibitory potential of the gold NHC complexes. Auranofin was used as a positive control and inhibited both enzymes effectively in the nanomolar range. Its activity against the mammalian enzyme (0.016 μM) is in good agreement with previous reports.[6k, 14] TrxR from *E. coli* was inhibited by Auranofin with a more than 15-fold higher IC_{50} value, which is most likely related to the fact that in contrast to their mammalian counterparts, bacterial TrxRs do not contain a very "aurophilic" selenocysteine residue in their active site.[15]

Gold(I) NHC complexes **1** and **5a-g** turned out to be quite effective inhibitors of both mammalian (IC_{50} values 0.04 – 0.40 μM) as well as bacterial TrxR (IC_{50} values: 0.11 – 0.55 μM). Similar to the results obtained with Auranofin, the mammalian form was stronger inhibited than the bacterial one. There was a clear preference for complexes **5a**, **5b** and **5d** with respect to the inhibition of mammalian TrxR (IC_{50} values close to 0.04 μM). The differences in the IC_{50} values against *E. coli* TrxR, ranging between 0.1 and 0.5 μM, were less marked. Here the most active complexes were the species with halogene-free NHC ligands **1**, **5c** and **5e**. An overall comparison of the results suggests that introduction of halogens in the NHC backbone had a positive effect in case of rat TrxR, but a negative effect in case of *E. coli* TrxR (compare **1** with **5a**/**5b**, **5c** with **5d** and **5e** with **5f**/**5g**).

Compound	rat TrxR IC_{50} [μM]	*E. coli* TrxR IC_{50} [μM]
Auranofin	0.016 +/-0.003	0.296 +/-0.069
4a-g	> 100	> 100
1	0.361 Ref. [6k]	0.134 +/-0.029
5a	0.043 +/-0.002	0.408 +/-0.040
5b	0.042 +/-0.006	0.442 +/-0.017
5c	0.209 +/-0.059	0.108 +/-0.028
5d	0.038 +/-0.010	0.309 +/-0.013
5e	0.244 +/-0.049	0.134 +/-0.031
5f	0.174 +/-0.027	0.228 +/-0.040
5g	0.098 +/-0.020	0.446 +/-0.029

Table 3: IC_{50} values of rat TrxR and *E.coli* TrxR inhibition tests. Standard errors are given as superscripts.

10.1002/chem.201604512

Discussion

Halogenated gold(I) NHC complexes can be prepared by established synthetic routes in high purities. The cytotoxicity screening of the complexes afforded IC_{50} values in the range of 4 – 17 μM. Stringent structure-activity relationships were not obvious in this assay due to the small differences in the respective IC_{50} values, although there was a certain trend for the fluorinated derivatives **5a** and **5f** and the phenylimidazole derived complex **5e**.

The phenylimidazole derived complexes **5e**-**f** as examples with high cytotoxicity were investigated for their cellular uptake. The accumulation in the cells was negatively affected by the presence of serum in the cell culture media, and this effect was most marked with **5f** and **5g**. The cellular fluorine concentrations were determined by HR-CS MAS and showed high levels when the cells were incubated with **5f**. Cellular fluorine and gold determined with **5f** were higher than those of the reference compounds AuCl and **4f**. Taken together, this strongly suggests that the intact complex **5f**, or at least its intact Au-NHC fragment, enters the cells. However, the bioavailability and trafficking of the Au-NHC complex is at the end heavily affected by the competing protein binding and likely by interactions with components of cell culture media and cells. Of note, “naked” Au^+ cations are known to disproportionate unless they are coordinated to stabilizing ligands.[16] This property might have hampered the cellular uptake of AuCl. Taking the volume and protein content of MCF-7 cells into account, the cellular molar concentration can be estimated from the measured nmol Au / protein values.[17] Based on this, complex **5f** (in serum containing media) reaches cellular gold levels of 77.1 μM after 1 hour. In relation to the exposure concentration (12 μM) this corresponds to an approximately 6-fold accumulation. The cellular levels of the compounds are thus sufficient to trigger pharmacological effects despite the impact of protein binding on cellular uptake.

The complexes were effective inhibitors of mammalian TrxR. The most active compounds in this assay were **5a**, **5b** and **5d**, suggesting a positive effect by introduction of fluorine or bromine in the NHC substructure. Concerning the application of the complexes as possible anticancer agents, the results therefore indicate a preference for the fluorine containing benzimidazole derivative **5a**, which triggers high cytotoxicity in combination with an efficient cellular uptake (see below) and TrxR inhibition.

For compound **5d**, the activity against drug resistant cell lines was proven and cellular uptake studies revealed that gold was accumulated to the same extent in drug resistant and drug sensitive cells. This indicates that gold(I) NHC complexes are not transported by the P-pg transporter and might open some opportunities for the application of the compounds in the treatment of resistant cancerous cells. This result could be of particular interest since not many details are known on the biological trafficking of anticancer gold(I) NHC complexes.

10.1002/chem.201604512

The determination of antibacterial effects against a panel of Gram-negative and Gram-positive strains demonstrated that all gold complexes in our study displayed a high activity (low micromolar range) towards the Gram-positive bacteria, but they were substantially lower active against the Gram-negative strains. Such a clear and consistent selectivity for Gram-positive strains has not been reported for previously investigated gold NHC complexes. Whereas some complexes of the type NHC-Au(I)-Cl had indeed triggered much stronger effects in Gram-positive bacteria[9e], this was not the case for other structural derivatives like cationic biscarbene[9b] derivatives. Hence, the here observed specific targeting of Gram-positive bacteria cannot be considered as a general effect of the gold(I) NHC center and likely depends on the type of used NHC and other ligands. For (non NHC) gold(I) complexes with phosphane ligands, the higher activity against Gram-positive bacteria appears to be more common, as summarized recently in a review paper by Glisic and Djuran [4e] Concerning Auranofin our study also showed a clear preference for Gram-positive strains, which had also been described previously.[10c] Differences in the relevance of TrxR for bacterial survival could be a possible explanation for the observed effects. In fact, many Gram-positive bacteria lack glutathione and are therefore highly dependent on a functional Trx/TrxR system.[18] In contrast, the inhibition of TrxR can be more effectively compensated by the glutathione / glutathione reductase system in Gram-negative bacteria. An alternative reason for the activity pattern may be a difference in uptake. Antibiotics against Gram-negative bacteria are generally more difficult to identify than those against Gram-positive bacteria, as reflected in current development pipelines.[19] A recent analysis of multiple screening projects suggests that this is due to the impaired ability to penetrate the Gram-negative cell wall with its additional outer membrane.[20],[21] Therefore, the determination of the intracellular concentrations of the NHC gold(I) complexes in Gram-positive vs. Gram-negative bacteria would be an attractive future extension of this work.

In contrast to the results obtained with mammalian TrxR, fluorine or bromine substituents on the NHC substructure had a negative effect on the efficacy of TrxR inhibition. Overall, **1** and **5c** represent the best combinations of low MIC and bacterial TrxR inhibition. Although the range of IC_{50} values was limited, we observed a diverging SAR for TrxR inhibition between the mammalian and the bacterial isoforms. This suggests that it may be possible to obtain gold(I) NHC-based inhibitors that are selective for the bacterial TrxR isoform, with a possibly enlarged split - unless other mechanisms also contribute - between cellular cytotoxicity and antibacterial potency. This fact is of particular interest since effective targeting of Trx/TrxR system in Gram-positive bacteria would represent a hitherto unexplored antibiotic mechanism.

10.1002/chem.201604512

Conclusions

In conclusion gold(I) NHC complexes of the type NHC-Au(I)-Cl represent a promising class of possible anticancer and antibacterial agents. Their cellular bioavailability is negatively affected by the presence of proteins in the culture media. However, sufficient amounts of the intact Au(I)-NHC fragment are taken up into the cells. Concerning the application as antitumor drugs, their activity against P-gp overexpressing cell lines is of high interest regarding the application in resistant malignancies. Antibacterial effects were especially pronounced in Gram-positive strains, which are highly dependent on an intact Trx/TrxR system due to a lack of glutathione. Structure-activity-relationships differed between antibacterial and antitumoral assays indicating options for the development of more selective agents in future studies.

Experimental Section

General

All reagents were obtained from Sigma-Aldrich or Fluka Analytical. The purities of the synthesized compounds were proven by elemental analysis (Flash EA 1112, Thermo Quest) and differed less than 0.5 % from the predicted values. ^{1}H NMR spectra, ^{13}C NMR spectra and ^{19}F NMR spectra were recorded using a Bruker AV II-400 or Bruker DRX-400 AS NMR spectrometer. Mass spectra were recorded on a Finnigan-MAT 95 spectrometer (ionisation energy for EI-MS: 70 eV). For the absorption measurements in both TrxR inhibition assays a Perkin Elmer 2030 Multilabel Reader VICTOR^{TM} X4 was used. The amount of gold and fluorine was detected by HR-CS AAS/MAS contrAA-700 from Analytik Jena. 1,3-Diethyl-benzimidazol-2-ium iodide and (1,3-diethyl-benzimidazol-2-ylidene)chloridogold(I) **1** were obtained as previously described.[6k]

Synthesis

Benzimidazoles

Halogenated benzimidazoles were prepared according to literature procedures[22]. The benzene-1,2-diamine precursors were dissolved in 40 mL formic acid and stirred under reflux conditions at 110 °C for 4h. Afterwards, the flask was cooled on ice, while neutralizing the solutions with concentrated ammonia. The water was evaporated, and the products were extracted from the white-grey ammonium formiate residue using dichloromethane (until the supernatant was colorless) as yellow solutions. Dichloromethane was evaporated and the pale yellow powders were dried under vacuum over 48h.

10.1002/chem.201604512

5-Fluoro-1*H*-benzimidazole[22-23]

see general procedure; starting material: 3,4-Diaminofluorobenzene (500.0 mg, 3.96 mmol), yield: 253.4 mg (1.86 mmol, 47 %), pale yellow powder; ^{1}H-NMR (400 MHz, $CDCl_3$-d_1) ∂ ppm 8.12 (s, 1H, BeIm-H2), 7.60 (ddd, $^{3}J_{H,H}$ = 8.8 Hz, $^{4}J_{H,F}$ = 4.7 Hz, $^{5}J_{H,H}$ = 0.6 Hz, 1H, BeIm-H7), 7.34 (ddd, $^{3}J_{H,F}$ = 9.6 Hz, $^{4}J_{H,H}$ = 2.5 Hz, $^{5}J_{H,H}$ = 0.6 Hz, 1H, BeIm-H4), 7.05 (ddd, $^{3}J_{H,F}$ = 9.7 Hz, $^{3}J_{H,H}$ = 8.8 Hz, $^{4}J_{H,H}$ = 2.5 Hz, 1H, BeIm-H6); ^{13}C-NMR (101 MHz, $CDCl_3$-d_1) ∂ ppm 159.8 (d, $^{1}J_{C,F}$ = 239.3 Hz, BeIm-C5$_{quat.}$), 141.3 (BeIm-C2H), 137.3 (BeIm-C3a$_{quat.}$), 134.1 (BeIm-C7a$_{quat.}$), 116.3 (d, $^{3}J_{C,F}$ = 10.2 Hz, BeIm-C7H), 111.7 (d, $^{2}J_{C,F}$ = 25.7 Hz, BeIm-C6H), 101.4 (d, $^{2}J_{C,F}$ = 26.0 Hz, BeIm-C4H); ^{19}F -NMR (1H) (376 MHz, $CDCl_3$-d_1) ∂ ppm -119.7 (td, $^{3}J_{F,H}$ = 9.3 Hz, $^{4}J_{F,H}$ = 4.7 Hz); elemental analysis $C_7H_5FN_2$ (calc. %/found %): C (61.76/61.51) H (3.70/3.86) N (20.58/20.39); MS (EI): m/z 136.1 $[M]^+$, 118.1 $[M\text{-}F+H]^+$.

5-Bromo-1*H*-benzimidazole

see general procedure; starting material: 4-Bromo-1,2-benzenediamine (500.0 mg, 2.67 mmol), yield: 268.3 mg (1.36 mmol, 51 %), pale yellow powder; ^{1}H-NMR (400 MHz, $CDCl_3$-d_1) ∂ ppm 8.10 (s, 1H, BeIm-H2), 7.82 (dd, $^{4}J_{H,H}$ = 1.7 Hz, $^{5}J_{H,H}$ = 0.5 Hz, 1H, BeIm-H4), 7.54 (dd, $^{3}J_{H,H}$ = 8.6 Hz, $^{5}J_{H,H}$ = 0.6 Hz, 1H, BeIm-H7), 7.41 (dd, $^{3}J_{H,H}$ = 8.6 Hz, $^{4}J_{H,H}$ = 1.8 Hz, 1H, BeIm-H6); ^{13}C-NMR (101 MHz, $CDCl_3$-d_1) ∂ ppm 141.2 (BeIm-C2H), 138.8 (BeIm-C3a$_{quat.}$), 136.5 (BeIm-C7a$_{quat.}$), 126.3 (BeIm-C6H), 118.5 (BeIm-C4H), 116.8 (BeIm-C7H), 116.2 (BeIm-C5Br$_{quat.}$); elemental analysis: $C_7H_5BrN_2$ (calc. %/found %): C (42.67/42.80), H (2.56/2.46), N (14.22/13.89); MS (EI): m/z 196.0 $[M]^+$, 117.0 $[M\text{-}Br+H]^+$, 116.0 $[M\text{-}Br]^+$

(Benz-/Phenyl-)imidazolium iodides 4a-g

The respective precursor (benz-/phenyl-)imidazoles were dissolved in 20 mL acetonitrile, 1 equivalent K_2CO_3 and 3 equivalents ethyl iodide were added. The reaction was stirred under reflux conditions for 24h (**4a-d**) or 28d (**4e-g**) at 110 °C. The solvent was evaporated and the residue was treated with 20 mL dichloromethane. The suspension was filtered to remove the excess of K_2CO_3 and the solvent was evaporated again. The residue was washed with tetrahydrofuran until the supernatant was colorless to remove the alkylation reagent. The wet powder was dried using a rotary evaporator and further dried under vacuum for 48h.

1,3-Diethyl-5-fluoro-benzimidazolium iodide 4a

see general procedure; starting material: 5-Fluoro-1*H*-benzimidazole (500.0 mg, 3.67 mmol), yield: (963.5 mg, 3.01 mmol, 82 %), pale salmon powder; ^{1}H-NMR (400 MHz, $CDCl_3$-d_1) ∂ ppm 11.12 (s, 1H, BeIm-H2), 7.78 (ddd, $^{3}J_{H,H}$ = 9.0, $^{4}J_{H,F}$ = 4.1 Hz, $^{5}J_{H,H}$ = 0.7, 1H, BeIm-H7), 7.45 (m, 2H, BeIm-H4 + BeIm-H6), 4.71 (q, $^{3}J_{H,H}$ = 7.5 Hz, 2H, CH_2), 4.66 (q, $^{3}J_{H,H}$ = 7.4 Hz,

2H, CH_2), 1.78 (t, $^3J_{H,H}$ = 7.4 Hz, 3H, CH_3), 1.76 (t, $^3J_{H,H}$ = 7.5 Hz, 3H, CH_3); ^{13}C-NMR (101 MHz, $CDCl_3$-d_1) ∂ ppm 161.5 (d, $^1J_{C,F}$ = 251.0 Hz, BeIm-C5$F_{quat.}$), 142.6 (BeIm-C2H), 131.9 (d, $^3J_{C,F}$ = 12.7 Hz, BeIm-C3$a_{quat.}$), 127.7 (BeIm-C7$a_{quat.}$), 116.3 (d, $^2J_{C,F}$ = 26.3 Hz, BeIm-C4/6H), 114.7 (d, $^3J_{C,F}$ = 10.2 Hz, BeIm-C7H), 100.1 (d, $^2J_{C,F}$ = 28.1 Hz, BeIm-C4/6H), 45.5 (CH_2), 43.4 (CH_2), 14.9 (CH_3), 14.7 (CH_3); ^{19}F -NMR (1H) (376 MHz, $CDCl_3$-d_1) ∂ ppm -110.5 (td, $^3J_{F,H}$ = 8.6 Hz, $^4J_{F,H}$ = 4.1 Hz); elemental analysis: $C_{11}H_{14}FIN_2$ (calc. %/found %) C (41.27/41.42), H (4.41/4.27), N (8.75/8.55); MS (ESI): m/z 193.1 $[M\text{-}I]^+$.

5-Bromo-1,3-diethyl-benzimidazolium iodide 4b

see general procedure; starting material: 5-Bromo-1*H*-benzimidazole (500.0 mg, 2.54 mmol), pale salmon powder, yield: 677.5 mg (1.78 mmol, 70 %); ^{1}H-NMR (400 MHz, $CDCl_3$-d_1) ∂ ppm 11.14 (s, 1H, BeIm-H2), 7.91 (dd, $^4J_{H,H}$ = 1.6, $^5J_{H,H}$ = 0.6 Hz, 1H, BeIm-H4), 7.78 (dd, $^3J_{H,H}$ = 8.8, $^4J_{H,H}$ = 1.7 Hz, 1H, BeIm-H6), 7.68 (dd, $^3J_{H,H}$ = 8.8, $^5J_{H,H}$ = 0.6 Hz, 1H, BeIm-H7), 4.70 (q, $^3J_{H,H}$ = 7.4 Hz, 2H, CH_2), 4.67 (q, $^3J_{H,H}$ = 7.4 Hz, 2H, CH_2), 1.79 (t, $^3J_{H,H}$ = 7.4 Hz, 3H, CH_3), 1.78 (t, $^3J_{H,H}$ = 7.4 Hz, 3H, CH_3); ^{13}C-NMR (101 MHz, $CDCl_3$-d_1) ∂ ppm 142.3 (BeIm-C2H), 132.2 (BeIm-C3$a_{quat.}$), 130.7 (BeIm-C7H), 130.2 (BeIm-C7$a_{quat.}$), 120.8 (BeIm-C5$Br_{quat.}$), 116.1 (BeIm-C6H), 114.5 (BeIm-C4H), 43.4 (CH_2), 43.3 (CH_2), 14.8 (CH_3) 14.8 (CH_3); elemental analysis: $C_{11}H_{14}BrIN_2$ (calc. %/found %) C (34.67/34.89), H (3.70/3.42), N (7.35/6.96); MS (ESI): m/z 253.0 $[M\text{-}I]^+$.

1,3-Diethylimidazol-2-ium iodide 4c

see general procedure; starting material: 1*H*-imidazole (250.0 mg, 3.67 mmol), yield: 530.9 mg (0.95 mmol, 26 %), pale yellow powder; ^{1}H-NMR (400 MHz, $CDCl_3$-d_1) ∂ ppm 10.20 (m, 1H, Im-H2), 7.49 (d, $^4J_{H,H}$ = 1.7 Hz, 2H, Im-H4 + Im-H5), 4.45 (q, $^3J_{H,H}$ = 7.4 Hz, 4H, CH_2), 1.64 (t, $^3J_{H,H}$ = 7.4 Hz, 6H, CH_3) ; ^{13}C-NMR (101 MHz, $CDCl_3$-d_1) ∂ ppm 136.1 (Im-C2H), 121.8 (2C, Im-C4H + Im-C5H), 45.5 (2C, CH_2), 15.6 (2C, CH_3); elemental analysis: $C_7H_{13}IN_2$ (calc. %/found %) C (33.35/33.47), H (5.50/5.24), N (11.11/11.02); MS (ESI): m/z 125.1 $[M\text{-}I]^+$.

4-Bromo-1,3-diethyl-imidazolium iodide 4d

see general procedure; starting material: 5-Bromo-1*H*-imidazole (500.0 mg, 3.40 mmol), yield: 945.3 mg (2.86 mmol, 84 %), pale yellow powder; ^{1}H-NMR (400 MHz, $CDCl_3$-d_1) ∂ ppm: 10.49 (d, $^4J_{H,H}$ = 2.0, 1H, Im-H2), 7.64 (d, $^4J_{H,H}$ = 1.9 Hz, 1H, Im-H5), 4.52 (q, $^3J_{H,H}$ = 7.4 Hz, 2H, CH_2), 4.39 (q, $^3J_{H,H}$ = 7.4 Hz, 2H, CH_2), 1.66 (t, $^3J_{H,H}$ = 7.4 Hz, 3H, CH_3), 1.65 (t, $^3J_{H,H}$ = 7.3 Hz, 3H, CH_3); ^{13}C-NMR (101 MHz, $CDCl_3$-d_1) ∂ ppm 137.4 (Im-C2H), 122.0 (Im-C4$Br_{quat.}$), 107.6 (Im-C5H), 46.3 (CH_2), 44.8 (CH_2), 15.5 (CH_3), 15.2 (CH_3); elemental

analysis: $C_7H_{12}BrIN_2$ (calc. %/found %): C (25.40/25.50), H (3.65/3.54), N (8.46/8.30); MS (ESI): m/z 203.0 $[M-I]^+$.

1,3-Diethyl-4-phenylimidazol-2-ium iodide 4e

see general procedure; starting material: 4-Phenyl-1*H*-imidazole (250.0 mg, 1.73 mmol), yield: 369.1 mg (1.21 mmol, 70 %), pale yellow powder; ^{1}H-NMR (400 MHz, $CDCl_3$-d_1) ∂ ppm 10.44 (d, $^4J_{H,H}$ = 1.9 Hz, 1H, Im-H2), 7.53 (m, 3H, Ph-$H_{para+meta}$), 7.43 (m, 2H, Ph-H_{ortho}), 7.30 (d, $^4J_{H,H}$ = 1.8 Hz, 1H, Im-H5), 4.52 (q, $^3J_{H,H}$ = 7.4 Hz, 2H, CH_2), 4.32 (q, $^3J_{H,H}$ = 7.4 Hz, 2H, CH_2), 1.70 (t, $^3J_{H,H}$ = 7.3 Hz, 3H, CH_3), 1.52 (t, $^3J_{H,H}$ = 7.3 Hz, 3H, CH_3); ^{13}C-NMR (101 MHz, $CDCl_3$-d_1) ∂ ppm 136.6 (Im-C2H), 135.3 (Im-$C4_{quat.}$),130.8 (Ph-CH_{para}), 129.5 (4C, Ph-$CH_{meta+ortho}$), 124.8 (Ph-$C1_{quat.}$), 118.7 (Im-C5), 45.6 (CH_2), 43.3 (CH_2), 15.8 (CH_3), 15.5 (CH_3); elemental analysis: $C_{13}H_{17}IN_2$ (calc. %/found %) C (47.58/47.53), H (5.22/5.25), N (8.54/8.48); MS (ESI): m/z 201.1 $[M-I]^+$.

1,3-Diethyl-4-(4-fluorophenyl)-imidazolium iodide 4f

see general procedure; starting material: 4-(4-Fluorophenyl)-1*H*-imidazole (500.0 mg, 3.08 mmol), yield: 533.1 mg (1.54 mmol, 50 %), pale yellow powder; ^{1}H-NMR (400 MHz, $CDCl_3$-d_1) ∂ ppm 10.34 (d, $^4J_{H,H}$ = 1.9, 1H, Im-H2), 7.48 (m, 2H, Ph-H_{ortho}), 7.35 (d, $^4J_{H,H}$ = 1.8 Hz, 1H, Im-H5), 7.25 (m, 2H, Ph-H_{meta}), 4.51 (q, $^3J_{H,H}$ = 7.4 Hz, 2H, CH_2), 4.29 (q, $^3J_{H,H}$ = 7.3 Hz, 2H, CH_2), 1.68 (t, $^3J_{H,H}$ = 7.3 Hz, 3H, CH_3), 1.52 (t, $^3J_{H,H}$ = 7.3 Hz, 3H, CH_3); ^{13}C-NMR (101 MHz, $CDCl_3$-d_1) ∂ ppm 164.0 (d, $^1J_{C,F}$ = 253.1 Hz, Ph-$C4F_{quat./para}$), 136.5 (Im-C2H), 134.2 (Ph-$C1_{quat.}$), 131.8 (d, 2C, $^3J_{C,F}$ = 8.7 Hz, Ph-CH_{ortho}), 120.8 (d, Ph-C'$1_{quat.}$, $^4J_{C,F}$ = 3.6 Hz), 119.2 (Im-C5H), 116.9 (d, 2C, $^2J_{C,F}$ = 21.9 Hz, Ph-CH_{meta}), 45.6 (CH_2), 43.3 (CH_2), 15.7 (CH_3), 15.5 (CH_3); ^{19}F -NMR (1H) (376 MHz, $CDCl_3$-d_1) ∂ ppm -108.7 (tt, $^3J_{F,H}$ = 8.3 Hz, $^4J_{F,H}$ = 5.1 Hz); elemental analysis: $C_{13}H_{16}FIN_2$ (calc. %/found %) C (45.10/45.12), H (4.66/4.65), N (8.09/7.99); MS (ESI): m/z 219.1$[M-I]^+$.

4-(4-Bromophenyl)-1,3-diethyl-imidazolium iodide 4g

see general procedure; starting material: 4-(4-Bromophenyl)-1*H*-imidazole (500.0 mg, 2.24 mmol), yield: 419.5 mg (1.03 mmol, 46 %), pale yellow powder; ^{1}H-NMR (400 MHz, $CDCl_3$-d_1) ∂ ppm 10.38 (dd, $^4J_{H,H}$ = 1.8 Hz, 1H, Im-H2), 7.69 (m, 2H, Ph-H_{meta}), 7.35 (m, 3H, Ph-H_{ortho} + Im-H5), 4.51 (q, $^3J_{H,H}$ = 7.4 Hz, 2H, CH_2), 4.30 (q, $^3J_{H,H}$ = 7.3 Hz, 2H, CH_2), 1.68 (t, $^3J_{H,H}$ = 7.3 Hz, 3H, CH_3), 1.53 (t, $^3J_{H,H}$ = 7.3 Hz, 3H, CH_3); ^{13}C-NMR (101 MHz, $CDCl_3$-d_1) ∂ ppm 136.8 (Im-C2H), 134.1 (Im-$C4_{quat.}$), 132.8 (2C, Ph-CH_{meta}), 131.1 (2C, Ph-CH_{ortho}), 125.6 (Ph-$C1_{quat.}$), 123.7 (Ph-$C4Br_{quat./para}$), 119.1 (Im-C5H), 45.7 (CH_2), 43.5 (CH_2), 15.7 (CH_3), 15.5 (CH_3); elemental analysis: $C_{13}H_{16}BrIN_2$ (calc. %/found %) C (38.36/38.52), H (3.96/4.04), N (6.88/6.68); MS (ESI): m/z 279.0 $[M-I]^+$.

10.1002/chem.201604512

General Procedure for Synthesis of NHC-Au-Cl Complexes 5a-g

An amount of 0.29 – 0.91 mmol of the respective (benz)imidazolium iodide **4a-g** and 0.6 equivalents of silver oxide were dissolved in 20 mL dichloromethane and stirred over 2 - 4h at room temperature under light protection. Then 1.1 equivalents of chloro(dimethylsulfide) gold(I) were added. After 10d of further stirring at room temperature the complete reaction mixture was filtered over a celite column. The complexes were isolated by evaporating the filtrate and dried under vacuum at 50 °C over a period of 72h.

Chlorido(1,3-diethyl-5-fluoro-benzimidazol-2-ylidene)gold(I) 5a

see general procedure; starting material: 1,3-Diethyl-5-fluoro-benzimidazolium iodide **4a** (100.0 mg 0.31 mmol), yield: 114.5 mg (0.27 mmol, 87 %), pale yellow powder; ^{1}H-NMR (400 MHz, $CDCl_3$-d_1) ∂ ppm 7.43 (ddd, $^{3}J_{H,H}$ = 9.5, $^{4}J_{H,F}$ = 4.2 Hz, $^{5}J_{H,H}$ = 0.4 Hz, 1H, BeIm-H7), 7.20 (m, 2H, BeIm-H4 + BeIm-H6), 4.53 (q, $^{3}J_{H,H}$ = 7.4 Hz, 2H, CH_2), 4.50 (q, $^{3}J_{H,H}$ = 7.3 Hz, 2H, CH_2), 1.54 (t, $^{3}J_{H,H}$ = 7.3 Hz, 3H, CH_3), 1.53 (t, $^{3}J_{H,H}$ = 7.4 Hz, 3H, CH_3); ^{13}C-NMR (101 MHz, $CDCl_3$-d_1) ∂ ppm 178.9 (BeIm-C2$_{quat.}$), 160.4 (d, $^{1}J_{C,F}$ = 244.9 Hz, BeIm-C5$_{quat.}$), 133.3 (d, $^{3}J_{C,F}$ = 12.7 Hz, BeIm-C3a$_{quat.}$), 129.2 (BeIm-C7a$_{quat.}$), 112.7 (d, $^{2}J_{C,F}$ = 25.8 Hz, BeIm-C4/6H), 112.3 (d, $^{3}J_{C,F}$ = 10.0 Hz, BeIm-C7H), 98.6 (d, $^{2}J_{C,F}$ = 27.6 Hz, BeIm-C4/6H), 44.2 (CH_2), 44.1 (CH_2), 15.5 (CH_3), 15.3 (CH_3); ^{19}F -NMR (1H) (376 MHz, $CDCl_3$-d_1) ∂ ppm -116.31 (td, $^{3}J_{F,H}$ = 8.6 Hz, $^{4}J_{F,H}$ = 4.2 Hz; elemental analysis: $C_{11}H_{13}AuClFN_2$ (calc. %/found %) (C 31.11/30.62), H (3.09/2.76), N (6.60/6.34); MS (EI): m/z 424.0 $[M]^+$, 389.01 $[M\text{-}Cl]^+$

Chlorido(5-bromo-1,3-diethyl-benzimidazol-2-ylidene)gold(I) 5b

see general procedure; starting material: 5-Bromo-1,3-diethyl-benzimidazolium iodide **4b** (300.0 mg, 0.78 mmol), yield: 333.3 mg (0.69 mmol, 88 %), pale yellow powder; ^{1}H-NMR (400 MHz, $CDCl_3$-d_1) ∂ ppm 7.65 (dd, $^{4}J_{H,H}$ = 1.7, $^{5}J_{H,H}$ = 0.5 Hz, 1H, BeIm-H4), 7.55 (dd, $^{3}J_{H,H}$ = 8.7, $^{4}J_{H,H}$ = 1.7 Hz, 1H, BeIm-H6), 7.36 (dd, $^{3}J_{H,H}$ = 8.6, $^{5}J_{H,H}$ = 0.5 Hz, 1H, BeIm-H7), 4.52 (q, $^{3}J_{H,H}$ = 7.2 Hz, 2H, CH_2), 4.50 (q, $^{3}J_{H,H}$ = 7.2 Hz, 2H, CH_2), 1.54 (t, $^{3}J_{H,H}$ = 7.3 Hz, 3H, CH_3), 1.53 (t, $^{3}J_{H,H}$ = 7.2 Hz, 3H, CH_3); ^{13}C-NMR (101 MHz, $CDCl_3$-d_1) ∂ ppm 178.9 (BeImC2$_{quat.}$), 133.9 (BeImC3a$_{quat.}$), 131.8 (BeImC7a$_{quat.}$), 127.7 (BeImC7H), 118.0 (BeImC5Br$_{quat.}$), 114.5 (BeImC6H), 112.6 (BeImC4H), 44.2 (CH_2), 44.1 (CH_2), 15.5 (CH_3), 15.4 (CH_3); elemental analysis: $C_{11}H_{13}AuBrClN_2$ (calc. %/found %) C (27.21/26.80), H (2.70/2.58), N (5.77/5.42); MS (EI): m/z 484.0 $[M]^+$, 449.0 $[M\text{-}Cl]^+$.

Chlorido[1,3-diethyl-imidazol-2-ylidene]gold(I) 5c

see general procedure; starting material: 1,3-diethyl-imidazol-2-ium iodide **4c** (240.0 mg, 0.95 mmol), yield: 269.9 mg (0.76 mmol, 80 %), pale grey powder; ^{1}H-NMR (400 MHz,

$CDCl_3$-d_1) ∂ ppm 6.96 (s, 2H, Im-H4 + Im-H5), 4.23 (q, $^3J_{H,H}$ = 7.3 Hz, 4H, CH_2), 1.47 (t, $^3J_{H,H}$ = 7.3 Hz, 6H, CH_3) ; ^{13}C-NMR (101 MHz, $CDCl_3$-d_1) ∂ ppm 169.8 (Im-C2H), 119.9 (2C, Im-C4H + Im-C5H), 46.5 (2C, CH_2), 16.5 (2C, CH_3); elemental analysis: $C_7H_{12}AuClN_2$ (calc. %/found %) C (7.86/7.64), H (3.39/3.27), N (7.86/7.64); MS (ESI): m/z 356.0 $[M]^+$, 321.1 $[M-Cl]^+$.

Chlorido(4-bromo-1,3-diethyl-imidazol-2-ylidene)gold(I) 5d

see general procedure; starting material: 4-Bromo-1,3-diethyl-imidazolium iodide **4d** (300.0 mg, 0.91 mmol), yield: 325 mg (0.75 mmol, 82 %), orange-brown powder; ^{1}H-NMR (400 MHz, $CDCl_3$-d_1) ∂ ppm 6.98 (s, 1H, Im-H5), 4.29 (q, $^3J_{H,H}$ = 7.2 Hz, 2H, CH_2), 4.24 (q, $^3J_{H,H}$ = 7.2 Hz, 2H, CH_2), 1.48 (t, $^3J_{H,H}$ = 7.4 Hz, 3H, CH_3), 1.45 (t, $^3J_{H,H}$ = 7.3 Hz, 3H, CH_3); ^{13}C-NMR (101 MHz, $CDCl_3$-d_1) ∂ ppm 171.8 (Im-$C2_{quat.}$), 120.1 (Im-$C4Br_{quat.}$), 104.7 (Im-C5H), 47.4 (CH_2), 45.8 (CH_2), 16.3 (CH_3), 16.1 (CH_3); elemental analysis: $C_7H_{11}AuBrClN_2$ (calc. %/found %) C (19.31/19.06), H (2.55/2.16) N (6.43/5.99); MS (EI): m/z 433.9 $[M]^+$, 399.0 $[M-Cl]^+$.

Chlorido[1,3-diethyl-4-phenylimidazol-2-ylidene]gold(I) 5e

see general procedure; starting material: 1,3-Diethyl-4-phenylimidazol-2-ium iodide **4e** (240.0 mg, 0.73 mmol), yield: 263.0 mg (0.64 mmol, 83 %), light red-brown powder; ^{1}H-NMR (400 MHz, $CDCl_3$-d_1) ∂ ppm 7.49 (m, 3H, Ph-$H_{para+meta}$), 7.36 (m, 2H, Ph-H_{ortho}), 6.90 (s, 1H, ImH5), 4.32 (q, $^3J_{H,H}$ = 7.4 Hz, 2H, CH_2), 4.21 (q, $^3J_{H,H}$ = 7.2 Hz, 2H, CH_2), 1.52 (t, $^3J_{H,H}$ = 7.3 Hz, 3H, CH_3), 1.32 (t, $^3J_{H,H}$ = 7.2 Hz, 3H, CH_3); ^{13}C-NMR (101 MHz, $CDCl_3$-d_1) ∂ ppm 170.3 (Im-$C2_{quat.}$), 134.5 (Im-$C4_{quat.}$), 129.7 (Ph-$C4H_{para}$), 129.3 (4C, Ph-$CH_{meta+ortho}$), 127.7 (Ph-$C1_{quat.}$), 117.7 (Im-C5), 46.8 (CH_2), 44.0 (CH_2), 17.0 (CH_3), 16.5 (CH_3); elemental analysis: $C_{13}H_{16}IAuClN_2$ (calc. %/found %) C (36.09/36.61), H (3.73/3.66), N (6.47/6.30); MS (ESI): m/z 432.0 $[M]^+$, 397.1 $[M-Cl]^+$.

Chlorido[1,3-diethyl-4-(4-fluorophenyl)-imidazol-2-ylidene]gold(I) 5f

see general procedure; starting material: 1,3-Diethyl-4-(4-fluorophenyl)imidazolium iodide **4f** (100.0 mg, 0.29 mmol), yield: 101.8 mg (0.23 mmol, 78 %); yellow powder; ^{1}H-NMR (400 MHz, $CDCl_3$-d_1) ∂ ppm 7.35 (m, 2H, Ph-H_{ortho}), 7.19 (m, 2H, Ph-H_{meta}), 6.90 (s, 1H, Im-H5), 4.27 (q, $^3J_{H,H}$ = 7.3 Hz, 2H, CH_2), 4.18 (q, $^3J_{H,H}$ = 7.2 Hz, 2H, CH_2), 1.52 (t, $^3J_{H,H}$ = 7.3 Hz, 3H, CH_3), 1.31 (t, $^3J_{H,H}$ = 7.2 Hz, 3H, CH_3); ^{13}C-NMR (101 MHz, $CDCl_3$-d_1) ∂ ppm 170.5 (Im-$C2_{quat.}$), 165.8 (d, $^1J_{C,F}$ = 251.5 Hz, Ph-C4 $_{quat./para}$), 133.4 (Im-$C4_{quat.}$), 131.4 (d, 2C, $^3J_{C,F}$ = 8.4 Hz, Ph-CH_{ortho}), 123.7 (d, 1C, $^4J_{C,F}$ = 3.7 Hz, Ph-$C1_{quat.}$), 117.9 (Im-C5H), 116.3 (d, $^2J_{C,F}$ = 21.9 Hz, Ph-CH_{meta}), 46.8 (CH_2), 44.0 (CH_2), 16.9 (CH_3), 16.4 (CH_3); ^{19}F -NMR (1H) (376 MHz, $CDCl_3$-d_1) ∂ ppm -110.7 (tt, $^3J_{F,H}$ = 8.3 Hz, $^4J_{F,H}$ = 5.2 Hz, 1F); elemental analysis:

10.1002/chem.201604512

$C_{13}H_{15}AuClFN_2$ (calc. %/found %) C (34.65/34.44), H (3.35/3.31), N (6.22/6.06); MS (EI): m/z 450.0 $[M]^+$, 415.1 $[M\text{-}Cl]^+$.

Chlorido[4-(4-bromophenyl)-1,3-diethyl-imidazol-2-ylidene]gold(I) 5g

see general procedure; starting material: 4-(4-Bromophenyl)-1,3-diethyl-imidazolium iodide **4g** (300.0 mg, 0.74 mmol), yield: 325.6 mg (0.64 mmol, 86 %), yellow powder; ^{1}H-NMR (400 MHz, $CDCl_3$-d_1) ∂ ppm 7.63 (m, 2H, Ph-H_{meta}), 7.23 (m, 2H, Ph-H_{ortho}), 6.91 (s, 1H, Im-H5), 4.24 (q, $^3J_{H,H}$ = 7.3 Hz, 2H, CH_2), 4.19 (q, $^3J_{H,H}$ = 7.3 Hz, 2H, CH_2), 1.52 (t, $^3J_{H,H}$ = 7.3 Hz, 3H, CH_3), 1.32 (t, $^3J_{H,H}$ = 7.2 Hz, 3H, CH_3); ^{13}C-NMR (101 MHz, $CDCl_3$-d_1) ∂ ppm 170.9 (Im-$C2_{quat.}$), 133.3 (Im-$C4_{quat.}$), 132.4 (2C, Ph-CH_{meta}), 130.4 (2C, Ph-CH_{ortho}), 126.5 (Ph-$C1_{quat.}$), 124.3 (Ph-$C4Br_{quat./para}$), 117.9 (Im-C5H), 46.8 (CH_2), 44.1 (CH_2), 16.9 (CH_3), 16.4 (CH_3); elemental analysis: $C_{13}H_{15}AuBrClN_2$ (calc. %/found %) C (30.52/30.35), H (2.96/2.65), N (5.48/5.30); MS (EI): m/z 510.0 $[M]^+$, 475.0 $[M\text{-}Cl]^+$

Cell Culture

HT-29 colon carcinoma cells, MDA-MB-231 breast cancer cells, MCF-7 breast carcinoma cells were maintained in Dulbecco's Modified Eagle Medium (4.5 g/L D-Glucose, L-Glutamine, Pyruvate), which was supplemented with gentamycin (50 mg/L) and fetal bovine serum superior, standardized (Biochrom GmbH, Berlin) (10 % V/V), and were passaged once a week. RC-124 healthy human kidney cells were maintained in McCoy's 5A (modified, with L-Glutamine) medium which was supplemented with gentamycin (50 mg/L) and fetal bovine serum superior, standardized (Biochrom GmbH, Berlin) (10 % V/V), and were also passaged once a week. For experiments with RC-124 cells, microtiter plates had been pretreated in the following way: 30 µL of a sterilized gelatin solution (1.5 % (m/V)) were added to each well of flat bottom 96-well plates, the plates were covered with their lids, incubated for 1h at 37 °C, the excess solution was removed, the wells were washed with PBS 7.4 pH, and the new cell-culture medium was added. Leukemic B-cell precursor (Nalm-6) and its vincristin (Nalm-6-VCR) and daunorubicin (Nalm-6-DNR) resistant sublines were cultured in RPMI 1640 supplemented with 10 % fetal calf serum.

Antiproliferative Assay in Tumorigenic and Non-tumorigenic Cells

The antiproliferative effects were determined according to a recently used method with minor modifications.[6b, k] In short: a volume of 100 µL of HT-29 cells (2565 cells/mL), MDA-MB-231 cells (4120 cells/mL), MCF-7 cells (4840 cells/mL) or RC-124 cells (1460 cells/mL) was transferred into the wells of 96-well plates (note: for RC-124 pretreated plates were used, see above) and incubated at 37 °C / 5 % CO_2 for 72h (MCF-7, MDA-MB-231, RC-124) or 48h (HT-29). Stock solutions of the compounds in dimethylformamide (DMF) were freshly

prepared and diluted with the respective cell culture medium to graded concentrations (final concentration of DMF: 0.1% V/V). After 72h (HT-29) or 96h (MCF-7, MDA-MB-231, RC-124) of exposure, the cell biomass was determined by crystal violet staining and the IC_{50} value was determined as the concentration that caused 50 % inhibition of cell proliferation compared to an untreated control. Results were calculated as the mean values of three independent experiments.

Protein Binding

The precipitation assay, based on a method of Ma et al.[24] was modified and performed with solutions containing bovine serum albumin or with fetal calf serum. A volume of 11 mL DMEM cell culture medium was supplemented with 1.1 mL FCS (standardized) or with 440 mg BSA. A volume of 1.0 mL of the corresponding solution was used for matrix matched calibration and was treated like the other samples without incubation. Stock solutions of the test compounds in DMF or DMSO (concentration: 12 mM) were prepared. A volume of 10 µL of each solution was pipetted into 10 mL of cell culture medium containing either FCS or BSA and mixed carefully (final incubation concentration: 12 µM). The reaction mix was incubated at 37 °C for 48h under shaking. After the desired period of time (0, 1, 4, 8, 24, 48h) 250 µL aliquots of every sample were treated with 500 µL of ice-cooled ethanol and stored at -25 °C for 2h. Afterwards the samples were centrifuged (2800 rpm at 4 °C for 15 min). A volume of 350 µL of the supernatant was separated and stored at -25°C. The experiment was carried out in duplicate. To 100 µL of each sample 10 µL of nitric acid (13 %) were added for stabilization and the gold content of the samples was quantified by HR-CS AAS (see below).

Cellular Uptake Studies

The cellular metal uptake was determined according to previously described methods.[6h, 25] In short: Uptake into MCF-7 cells: MCF-7 breast carcinoma cells were grown until at least 75-80 % confluency in 150 cm^2 cell-culture flasks. Stock solutions of the compounds in DMF were prepared and diluted with cell culture medium to a final concentration of 12.0 µM immediately before use (final DMF concentration: 0.1 % V/V). The cell culture medium of the flasks was replaced with the medium that contained the metal compound (20 mL) and the flasks were incubated at 37 °C / 5 % CO_2 up to 24h. After the desired incubation period the uptake was stopped by removing cell culture media. The cells were washed with PBS (10 mL), the washing solution was removed, and the cells were isolated after 6 min trypsinization (2.4 mL trypsin solution 0.05 %, containing EDTA 0.004 %) by centrifugation (5 min, 3.5 rpm). Nalm-6 cells and resistant Nalm-6 cells: Cells exposed to **5d** were isolated by centrifugation. The obtained cell pellets were stored at –20 °C for further use. For metal and protein quantification the pellets were resuspended in demineralized water (1.0 mL) and

10.1002/chem.201604512

lysed 30 min by ultra-sonication. The protein content of lysates was determined by the Bradford method and the gold and fluorine content was determined as described below. The final results of gold and fluorine concentrations were calculated from data obtained in two or three independent experiments and are expressed as nmol of gold or fluorine per mg cellular protein.

HR-CS AAS and HR-CS MAS

For the gold and fluorine measurements a contrAA 700 high-resolution continuum-source atomic absorption spectrometer (Analytik Jena AG) was used. Pure samples of the respective complexes were used as standards and calibration was done in a matrix-matched manner. The mean integrated absorbance of triple injections were used throughout the studies.

Gold: Triton-X 100 (1 %, 10 µL) as well as ascorbic acid (1 %, 10µL), were directly added to each standard sample (100 µL). Samples were injected (25 µL) into coated standard graphite tubes (Analytik Jena AG) and thermally processed as previously described in more detail with some appropriate modifications in the temperature program (see below). Drying steps were adjusted and the atomization temperature set to 1850 °C. Gold was quantified at a wavelength of 242.7950 nm.[17a, 25]

Steps	Temp. [°C]	Ramp [°C/s]	Hold [s]
Drying	80	8	20
Drying	90	3	20
Drying	110	5	10
Drying	350	50	15
Pyrolysis	700	200	20
Gas adaption	700	0	5
Atomize	1850	1500	6
Clean	2550	500	6

Table 4: Modified temperature program for HR-CS AAS gold quantification

Fluorine: Measurements were performed according to a previously described method with some appropriate modifications.[12c] Triton-X 100 (1 %, 10 µL) was added to each sample (100 µL). A volume of 20 µL was injected into coated standard graphite tubes (Analytik Jena AG, Germany), which contained a tantalum foil of 0.05 mm thickness (Sigma-Aldrich, Germany), and was processed as outlined in table 5. Drying, cooling and cleaning steps

10.1002/chem.201604512

were adjusted in comparison to the reported method[12c] and the concentrations of the gallium nitrate modifier solution were changed. Fluorine was quantified as GaF at a wavelength of 211.2480 nm.

Steps	Temp. [°C]	Ramp [°C/s]	Hold [s]	Pretreat/Modifier $Ga(NO_3)_3$
Drying	120	30	5	2 µL 5.0 g/L
Cooling	80	NP	1	
Drying	90	6	45	5 µL 7.5 g/L
Drying	120	6	20	
Drying	300	20	3	
Pyrolysis	520	200	10	
Gas adaption	520	0	5	
Vaporization	1200	800	7	
Cleaning	2500	1000	4	

Table 5: Modified temperature program for HR-CS MAS fluorine quantification

Apoptosis Induction in Drug Resistant Nalm-6 Cells

Measurement of DNA fragmentation in Nalm-6 cells: Apoptotic cell death was determined by a modified cell cycle analysis, which detects DNA fragmentationat at the single-cell level. For measurement of DNA fragmentation cells were seeded at adensity $1x10^5$ cells mL^{-1} and treated with different concentrations of **5d**. After 72h of incubation, cells were collected by centrifugation at 300 g for 5 min, washed with PBS at 4 °C and fixed in PBS/formaldehyde (2 %, V/V) on ice for 30 min. After fixation, cells were incubated with ethanol/PBS (2:1, V/V) for 15 min, pelleted, and resuspended in PBS containing RNase A (40 mg/mL). After incubation for 30 min at 37 °C, cells were pelleted again and finally resuspended in PBS containing propidium iodide (50 mg/mL). Nuclear DNA fragmentation was then quantified by flow cytometric determination of hypodiploid DNA. Data were collected and analyzed by using a FACScan (Becton Dickinson, Heidelberg, Germany) equipped with the CELLQuest software. Data are given in % hypoploidy (subG1), which reflects the number of apoptotic cells.

Antibacterial Screening

The following strains were used and maintained at 37 °C in MH (21 g/L Müller-Hinton, 1 % glucose, pH 7.4) or TSY (30 g/L Trypticase soy broth, 3 g/L Yeast extract, pH 7.0-7.2) medium: Acinetobacter baumannii (DSM 30007, ATCC 19606) in MH, Enterobacter cloacae (DSM 46481, ATCC 23355) in MH, Escherichia coli (DSM 1116, ATCC 9637) in TSY,

10.1002/chem.201604512

Klebsiella pneumoniae (DSM 11678, ATCC 33495) in MH, Pseudomonas aeruginosa PA7 (DSM 24068) in MH, Enterococcus faecium (DSM 20477, ATCC 19434) in TSY, Staphylococcus aureus MRSA (DSM 11822, ICB 25701) in TSY, Staphylococcus aureus MRSA (clinical isolate, RKI 11-02670) in TSY. The determination of minimum inhibitory concentration (MIC) values was carried out following a standardized protocol in broth dilution assays.[26] Compounds were serially diluted starting from 100 µM with the exception of Auranofin, that was serially diluted from 50 µg/mL. Starting inocula of 2-8x10^5 colony forming units/ml (CFU/mL) in MH or TSY medium at 37°C were used and serial dilutions were carried out in 96-well microtiter plates in duplicate. After an incubation of the plates for 20h at 37 °C, the absorbance at 600 nm was measured to determine the MIC value. The MIC values for the tested compounds were determined in two independent experiments. Amikacin (*P. aeruginosa*), Linezolid (*S. aureus*), and Ciprofloxacin (all other strains) served as positive controls.

Inhibition of mammalian TrxR

To determine the inhibition of mammalian TrxR an established microplate reader based assay was performed. For this purpose, commercially available rat liver TrxR (from Sigma-Aldrich) was used and diluted with distilled water to achieve a concentration of 3.58 U/mL. The compounds were freshly dissolved as stock solutions in DMF. 25 µL aliquots of the enzyme solution and 25 µL of either potassium phosphate buffer pH 7.0 containing the compounds in graded concentrations or 25 µL buffer without compounds but DMF (positive control) were added. 50 µL of a blank solution (DMF in buffer) was also prepared (final concentrations of DMF: 0.5 % V/V). The resulting solutions were incubated with moderate shaking for 75 min at 37 °C in a 96-well plate. To each well, 225 µL reaction mixture (1 mL reaction mixture consists of 500 µL potassium phosphate buffer pH 7.0, 80 µL EDTA solution (100 mM, pH 7.5), 20 µL BSA solution (0.2 %), 100 µL of NADPH solution (20 mM) and 300 µL distilled water) were added and the reaction started immediately by addition of 25 µL of an 20 mM ethanolic DTNB solution. After proper mixing, the formation of 5-TNB was monitored with a microplate reader at 405 nm 10 times in 35 s intervals for about 6 min. The increase in 5-TNB concentration over time followed a linear trend ($r^2 \geq 0.990$), and the enzymatic activities were calculated as the slopes (increase in absorbance per second) thereof. For each tested compound, the noninterference with the assay components was confirmed by a negative control experiment using an enzyme-free test solution. The IC_{50} values were calculated as the concentration of compound decreasing the enzymatic activity of the untreated control by 50 % and are given as the means and error of three repeated experiments.

10.1002/chem.201604512

TrxR *E.coli* Inhibition Assay

The DTNB coupled thioredoxin reductase inhibition assay for *E.coli* was partly adopted and modified from Lu at al.[18b] Commercially available *E.coli* TrxR and its natural substrate *E.coli* Trx (both from Sigma-Aldrich) were used and diluted with distilled water to achieve a concentration of 35.5 U/mL for the enzyme and 0.77 µg/mL for the substrate. The compounds were freshly dissolved as stock solutions in DMF. 10 µL aliquots of the enzyme solution, 10 µL substrate solution, 100 µL NADPH (200 mM) in TE buffer were mixed in a well with 20 µL TE buffer pH 7.5 (consists of Tris-HCl 50 mM and EDTA 1 mM in aqueous solution) containing the compounds in graded concentrations or 20 µL buffer solution without compounds (control). Blank solutions: 100 µL NADPH (200 mM) and 40 µL of a DMF/buffer mixture were added and the resulting solutions were incubated with moderate shaking for 75 min at 25 °C in a 96-well plate (final concentrations of DMF: 0.5 % V/V). To each well, 100 µL of reaction mixture (containing NADPH 200 µM and DTNB 5 mM in TE buffer solution) were added and the reaction started immediately. After proper mixing, the formation of 5-TNB was monitored with a microplate reader (Perkin-Elmer Victor X4) at 405 nm 10 times in 35 s intervals for about 6 min. The values were corrected using the absorbances of the blank solution. The increase in 5-TNB concentration over time followed a linear trend ($r^2 \geq 0.990$), and the enzymatic activities were calculated as the slopes (increase in absorbance per second) thereof. For each tested compound, the noninterference with the assay components was confirmed by a negative control experiment, where the highest test compound concentration is used and the enzyme aliquot solution is replaced by the same amount of TE buffer. The IC_{50} values were calculated as the concentration of compound decreasing the enzymatic activity of the positive control by 50 % and are given as the means and error of three repeated experiments.

Acknowledgements

We thank Galina Sergeev for initial antibacterial measurements.

Supporting information

Results of apoptosis induction in melanoma cells and a table with MIC values expressed as mass concentrations are provided.

Abbreviations

HR-CS AAS: high resolution continuum source atomic absorption spectroscopy

HR-CS MAS: high resolution continuum source molecule absorption spectroscopy

MIC: minimal inhibitory concentration

NHC: *N*-heterocyclic carbene

TrxR: thioredoxin reductase

References

[1] a) R. Rubbiani, B. Wahrig and I. Ott, *J. Biol. Inorg. Chem.* **2014**, *19*, 961-965; b) W. F. Kean and I. R. Kean, *Inflammopharmacology* **2008**, *16*, 112-125.
[2] R. Koch, *Verhandlungen des X. Internationalen Medizinischen Kongresses, Berlin 1890. 1891 Bd.I. Verlag von August Hirschwald, Berlin* **1890**.
[3] M. L. Healy, K. K. Lim and R. Travers, *Int. J. Rheum. Dis.* **2009**, *12*, 145-148.
[4] a) I. Ott, *Coord. Chem. Rev.* **2009**, *253*, 1670-1681; b) S. Nobili, E. Mini, I. Landini, C. Gabbiani, A. Casini and L. Messori, *Med. Res. Rev.* **2010**, *30*, 550-580; c) B. Bertrand and A. Casini, *Dalton Trans.* **2014**, *43*, 4209-4219; d) S. J. Berners-Price and A. Filipovska, *Metallomics* **2011**, *3*, 863-873; e) B. D. Glisic and M. I. Djuran, *Dalton Trans.* **2014**, *43*, 5950-5969.
[5] a) L. Oehninger, R. Rubbiani and I. Ott, *Dalton Trans.* **2013**, *42*, 3269-3284; b) A. Gautier and F. Cisnetti, *Metallomics* **2012**, *4*, 23–32.
[6] a) B. Bertrand, L. Stefan, M. Pirrotta, D. Monchaud, E. Bodio, P. Richard, P. Le Gendre, E. Warmerdam, M. H. de Jager, G. M. Groothuis, M. Picquet and A. Casini, *Inorg. Chem.* **2014**, *53*, 2296-2303; b) R. Rubbiani, L. Salassa, A. de Almeida, A. Casini and I. Ott, *ChemMedChem* **2014**, *9*, 1205-1210; c) P. Holenya, S. Can, R. Rubbiani, H. Alborzinia, A. Junger, X. Cheng, I. Ott and S. Wolfl, *Metallomics* **2014**, *6*, 1591-1601; d) X. Cheng, P. Holenya, S. Can, H. Alborzinia, R. Rubbiani, I. Ott and S. Wolfl, *Mol. Cancer* **2014**, *13*, 221; e) O. Rackham, A.-M. J. Shearwood, R. Thyer, E. McNamara, S. M. K. Davies, B. A. Callus, A. Miranda-Vizuete, S. J. Berners-Price, Q. Cheng, E. S. J. Arnér and A. Filipovska, *Free Radic. Biol. Med.* **2011**, *50*, 689-699; f) J. L. Hickey, R. A. Ruhayel, P. J. Barnard, M. V. Baker, S. J. Berners-Price and A. Filipovska, *J. Am. Chem. Soc.* **2008**, *130*, 12570-12571; g) R. Rubbiani, E. Schuh, A. Meyer, J. Lemke, J. Wimberg, N. Metzler-Nolte, F. Meyer, F. Mohr and I. Ott, *Med. Chem. Commun.* **2013**, *4*, 942-948; h) R. Rubbiani, S. Can, I. Kitanovic, H. Alborzinia, M. Stefanopoulou, M. Kokoschka, S. Monchgesang, W. S. Sheldrick, S. Wolfl and I. Ott, *J. Med. Chem.* **2011**, *54*, 8646-8657; i) M. Baker, P. J. Barnard, S. J. Berners-Price, S. K. Brayshaw, J. L. Hickey, B. W. Skelton and A. H. White, *Dalton Trans.* **2006**, 3708-3715; j) T. Zou, C. T. Lum, S. S.-Y. Chui and C.-M. Che, *Angew. Chem. Int. Ed. Engl.* **2013**, *52*, 1-5; k) R. Rubbiani, I. Kitanovic, H. Alborzinia, S. Can, A. Kitanovic, L. A. Onambele, M. Stefanopoulou, Y. Geldmacher, W. S. Sheldrick, G. Wolber, A. Prokop, S. Wolfl and I. Ott, *J. Med. Chem.* **2010**, *53*, 8608-8618; l) R. W.-Y. Sun, M. Zhang, D. Li, Z.-F. Zhang, H. Cai, M. Li, Y.-J. Xian, S. W. Ng and A. S.-T. Wong, *Chem. Eur. J.* **2015**, *21*, 18534 – 18538.
[7] A. Pratesi, C. Gabbiani, E. Michelucci, M. Ginanneschi, A. M. Papini, R. Rubbiani, I. Ott and L. Messori, *J. Inorg. Biochem.* **2014**, *136*, 161-169.
[8] a) E. Persch, O. Dumele and F. Diederich, *Angew. Chem. Int. Ed. Engl.* **2015**, *54*, 3290-3327; b) R. Wilcken, M. O. Zimmermann, A. Lange, A. C. Joerger and F. M. Boeckler, *J. Med. Chem.* **2013**, *56*, 1363-1388; c) S. Purser, P. R. Moore, S. Swallow and V. Gouverneur, *Chem Soc Rev* **2008**, *37*, 320-330; d) E. P. Gillis, K. J. Eastman, M. D. Hill, D. J. Donnelly and N. A. Meanwell, *J. Med. Chem.* **2015**, *58*, 8315-8359.
[9] a) G. A. Fernandez, M. S. Vela Gurovic, N. L. Olivera, A. B. Chopa and G. F. Silbestri, *J. Inorg. Biochem.* **2014**, *135*, 54-57; b) I. Özdemir, A. Denizci, H. T. Öztürk and B. Cetinkaya, *Appl. Organomet. Chem.* **2004**, *18*, 318-322; c) S. Ray, R. Mohan, J. K. Singh, M. K. Samantaray, M. M. Shaikh, D. Panda and P. Ghosh, *J Am Chem Soc* **2007**, *129*, 15042-15053; d) T. Samanta, G. Roymahapatra, W. F. Porto, S. Seth, S. Ghorai, S. Saha, J. Sengupta, O. L. Franco, J. Dinda and S. M. Mandal, *PLoS One* **2013**, *8*, e58346; e) I. Özdemir, N. Temelli, S. Günal and S. Demir, *Molecules* **2010**, *15*, 2203-2210; f) Öznur Dogan, N. Kaloglu, S. Demir, I. Özdemir, S. Günal and I. Özdemir, *Monatsh. Chem.* **2013**, *144*, 313-319; g) R. R. Butorac, S. S. Al-Deyab and A. H. Cowley, *Molecules* **2011**, *16*, 2285-2292; h) T. Bernardi, S. Badel, P. Mayer, J. Groelly, P. de Fremont, B. Jacques, P. Braunstein, M. L. Teyssot, C. Gaulier, F.

Cisnetti, A. Gautier and S. Roland, *ChemMedChem* **2014**, *9*, 1140-1144; i) L. Paloque, C. Hemmert, A. Valentin and H. Gornitzka, *Eur. J. Med. Chem.* **2015**, *94*, 22-29; j) C. Hemmert, A. Fabie, A. Fabre, F. Benoit-Vical and H. Gornitzka, *Eur. J Med. Chem.* **2013**, *60*, 64-75.
[10] a) A. Debnath, D. Parsonage, R. M. Andrade, C. He, E. R. Cobo, K. Hirata, S. Chen, G. Garcia-Rivera, E. Orozco, M. B. Martinez, S. S. Gunatilleke, A. M. Barrios, M. R. Arkin, L. B. Poole, J. H. McKerrow and S. L. Reed, *Nat. Med.* **2012**, *18*, 956-960; b) E. R. Sharlow, S. Leimgruber, S. Murray, A. Lira, R. J. Sciotti, M. Hickman, T. Hudson, S. Leed, D. Caridha, A. M. Barrios, D. Close, M. Grogl and J. S. Lazo, *ACS Chem. Biol.* **2014**, *9*, 663-672; c) M. B. Harbut, C. Vilcheze, X. Luo, M. E. Hensler, H. Guo, B. Yang, A. K. Chatterjee, V. Nizet, W. R. Jacobs, Jr., P. G. Schultz and F. Wang, *Proc. Natl. Acad. Sci. U S A* **2015**, *112*, 4453-4458; d) M. I. Cassetta, T. Marzo, S. Fallani, A. Novelli and L. Messori, *Biometals* **2014**, *27*, 787-791.
[11] a) M. Baker, P. J. Barnard, S. K. Brayshaw, J. L. Hickey, B. W. Skelton and A. H. White, *Dalton Trans.* **2005**, *37*, 37-42; b) P. Fremont, N. M. Scott, E. D. Stevens and S. P. Nolan, *Organometallics* **2005**, *24*, 2411-2418; c) L. Ray, V. Katiyar, S. Barman, M. J. Raihan, H. Nanavati, M. M. Shaikh and P. Ghosh, *J. Organomet. Chem.* **2007**, *692*, 4259-4269; d) H. M. J. Wang and I. J. B. Lin, *Organometallics* **1998**, *17*, 972-975.
[12] a) M. Krüger, M.-D. Huang, H. Becker-Roß, S. Florek, I. Ott and R. Gust, *Spectrochim. Acta, Part B* **2012**, *69*, 50-55; b) H. Gleisner, B. Welz and J. W. Einax, *Spectrochim. Acta B* **2010**, *65*, 864–869; c) I. Würtenberger and R. Gust, *Anal. Bioanal. Chem.* **2014**, *406*, 3431–3442.
[13] L. B. Rice, *Infect. Control Hosp. Epidemiol.* **2010**, *31 Suppl 1*, S7-10.
[14] a) S. Gromer, L. D. Arscott, C. H. Williams, R. H. Schirmer and K. Becker, *J. Biol. Chem.* **1998**, *273*, 20096–20101; b) M. P. Rigobello, G. Scutari, A. Folda and A. Bindoli, *Biochem. Pharmacol.* **2004**, *67*, 689–696; c) Y. Omata, M. Folan, M. Shaw, R. L. Messer, P. E. Lockwood, D. Hobbs, S. Bouillaguet, H. Sano, J. B. Lewis and J. C. Wataha, *Toxicol. In Vitro* **2006**, *20*, 882-890.
[15] B. W. Lennon, C. H. Williams, Jr. and M. L. Ludwig, *Protein Sci* **1999**, *8*, 2366-2379.
[16] T. Zou, C. T. Lum, C. N. Lok, J. J. Zhang and C. M. Che, *Chem. Soc. Rev.* **2015**.
[17] a) R. Gust, B. Schnurr, R. Krauser, G. Bernhardt, M. Koch, B. Schmid, E. Hummel and H. Schönenberger, *J. Cancer Res. Clin. Oncol.* **1998**, *124*, 585-597; b) H. Reile, G. Bernhardt, M. Koch, H. Schonenberger, M. Hollstein and F. Lux, *Cancer Chemother. Pharmacol.* **1992**, *30*, 113-122.
[18] a) R. C. Fahey, W. C. Brown, W. B. Adams and M. B. Worsham, *J. Bacteriol.* **1978**, *133*, 1126-1129; b) J. Lu, A. Vlamis-Gardikas, K. Kandasamy, R. Zhao, T. N. Gustafsson, L. Engstrand, S. Hoffner, L. Engman and A. Holmgren, *FASEB J* **2013**, *27*, 1394-1403; c) O. Uziel, I. Borovok, R. Schreiber, G. Cohen and Y. Aharonowitz, *J. Bacteriol.* **2004**, *186*, 326-334.
[19] M. S. Butler, M. A. Blaskovich and M. A. Cooper, *J. Antibiot.* **2013**, *66*, 571-591.
[20] D. G. Brown, T. L. May-Dracka, M. M. Gagnon and R. Tommasi, *J. Med. Chem.* **2014**, *57*, 10144-10161.
[21] R. Tommasi, D. G. Brown, G. K. Walkup, J. I. Manchester and A. A. Miller, *Nature Reviews Drug Discovery* **2015**, *14*, 529-542.
[22] a) B. K. Das, N. Shibata, K. Harada and T. Toru, *Arkivoc* **2007**, 73-82; b) G. Aridoss and K. K. Laali, *Eur. J. Org. Chem.* **2011**, 2827-2835.
[23] H. Thakuria and G. Das, *Arkivoc* **2008**, *15*, 321-328.
[24] J. Ma, G. Stoter, J. Verweij and J. H. Schellens, *Cancer Chemother. Pharmacol.* **1996**, *38*, 391-394.
[25] I. Ott, H. Scheffler and R. Gust, *ChemMedChem* **2007**, *2*, 702-707.
[26] DIN 58940-7: Medical microbiology - Susceptibility testing of microbial pathogens to antimicrobial agents - Determination of the minimum bactericidal concentration (MBC) with the method of microbouillondilution; German and English, **2009**.

10.1002/chem.201604512

Graphical Abstract